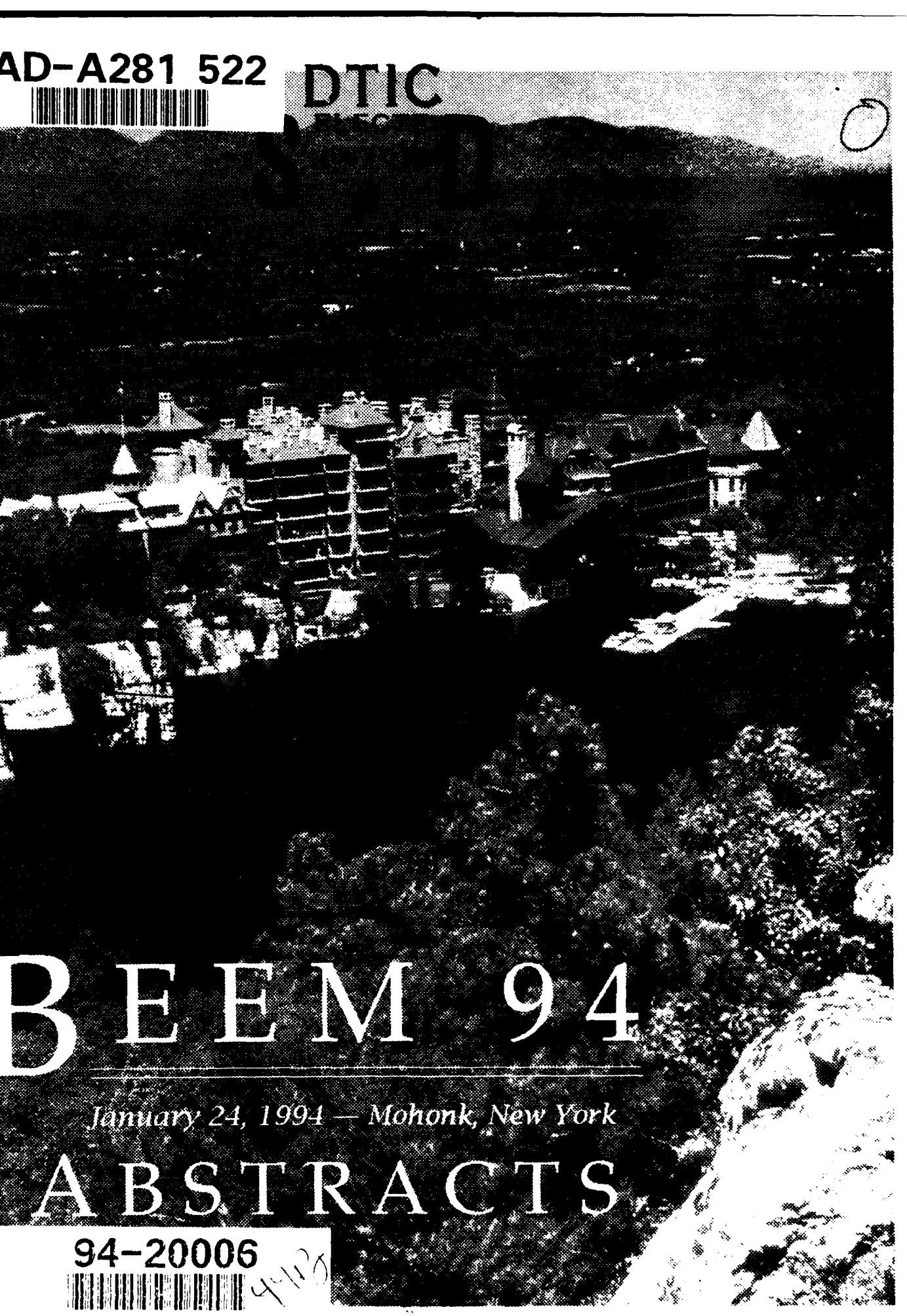

BEM 94

January 24, 1994 — Mohonk, New York

ABSTRACTS

BEEM 94

Mohonk, New York

FIFTH ANNUAL WORKSHOP ON BALLISTIC ELECTRON EMISSION MICROSCOPY

Mohonk Mountain House
January 24, 1994

Venkatesh Narayanamurti, Conference Chair
University of California, Santa Barbara

PROGRAM COMMITTEE

SPONSORED BY

Office of Naval Research

Ballistic Missile Defense Organization

American Vacuum Society
Electronic Materials & Processing Division

IN ASSOCIATION WITH PCSI-21
Donald J. Wolford
John D. Dow
Leo J. Schowalter

BEEM Publications Coordinated by **Leo J. Schowalter**

BEEM 94

January 24, 1994 — Mohonk, New York

Table of Contents

Cover: Mohonk Mountain House. From a photo by Matthew Seaman.

BEEM 94 *January 24, 1994 — Mohonk, New York*

January 24, 1994

Dear Attendee:

Welcome to the fifth BEEM Workshop at beautiful Lake Mohonk, Mohonk House, Mohonk, New York. I hope you will find the workshop enjoyable and rewarding.

This year's conference highlights recent research through 14 abstracts. The program committee, chaired by Mark Stiles, has put together an agenda which should allow time for oral presentation and discussion. Each talk, as in the last workshop, will also be displayed as a poster. I would like to thank the committee, and especially Mark and past chair Rudy Ludeke, for their diligent effort. On behalf of the Workshop I would also like to acknowledge the Office of Naval Research (ONR) and the Ballistic Missile Defense Organization (BMDO) for their financial support. I would also like to thank my assistant Kathy Kramer, and Sally Vito and Miki Swick of UCSB Conference Services, for their considerable and patient administrative support. Finally, I would like to thank Leo Schowalter for publications support.

Venky Narayanamurti

Conference Chair

BEEM 94 *January 24, 1994 — Mohonk, New York*

Workshop Program

8:15 Welcoming Remarks: ***Venky Narayanamurti***, Conference Chair, University of California, Santa Barbara

Session I ***Chair: R.A. Buhrman***, Cornell University

8:30 "Electron transport across interfaces and surfaces: an overview." ***Max Fischetti***, IBM Thomas J. Watson Research Center

9:20 "BEEM studies of strain-tuned semiconductor interfaces." ***S.J. Manion***, *L. D. Bell, W. J. Kaiser, A. M. Milliken, R. W. Fathauer, and M. H. Hecht,* Jet Propulsion Laboratories/California Institute of Technology

9:35 "Transport studies in semiconductor heterostructures using BEEM." ***T. Sajoto***, *J.J. O'Shea, S. Bhargava, D. Leonard, M.A. Chin, and V. Narayanamurti,* University of California, Santa Barbara

10:00 "Spectroscopic studies of quantum-wells and -wires using an STM." ***L. Samuelson***, *J. Lindahl, L. Montelius, and M.-E. Pistol*, Lund University

10:25 *BREAK*

Session II ***Chair: L.D. Bell***, Jet Propulsion Laboratories

10:55 "BEEM in pinholes of NiS_2 films on n-Si(111)-7x7: determination of the impact ionization quantum yield in Si." ***A. Bauer*** *and R. Ludeke,* Freie Universität Berlin

11:20 "Low-temperature UHV BEEM of epitaxial $CoSi_2$/Si(111)." *H. von Kaenel,* ***E.Y. Lee***, *and H. Sirringhaus,* ETH Hönggerberg

11:45 "Interfacial barrier studies of epitaxial CoGa on n-type (100) GaAs with BEEM." ***L. Tsau***, *T.C. Kuo, and K.L. Wang,* University of California, Los Angeles

12:00 "BEEM on Au/Si(111)7x7 and Au/CaF_2/Si(111)7x7." ***M.T. Cuberes***, *A. Bauer, H.J. Wen, M. Prietsch, and G. Kaindl,* Freie Universität Berlin

12:25 *LUNCH*

Session III ***Chair: T.K. Gaylord***, Georgia Institute of Technology

1:25 "Temperature dependence of Schottky barriers as probed by BEEM." ***S. Bhargava***, *J.J. O'Shea, T. Sajoto, D. Leonard, M.A. Chin, V. Narayanamurti, W.J. Kaiser, M.H. Hecht, L.D. Bell, S.J Manion, C.E. Bryson III, and M. Ackeret,* University of California, Santa Barbara

1:40 "Nanoscopic barrier height distributions at metal/semiconductor interfaces and observation of critical lengths." ***B.A. Morgan***, *K.M. Ring, W. Bi, C.W. Tu, K.L. Kavanagh, A.A. Talin, T. Ngo, and R.S. Williams,* University of California, San Diego

1:55 "BEEM studies of reversed-biased Schottky diodes." ***A. Davies*** *and H.G. Craighead*, Cornell University

2:10 "Ballistic models applied to low-temperature BEEM measurements of Au/Si interfaces." ***D. K. Gutbrie***, *G.N. Henderson, L.E. Harrell, P.N. First, T.K. Gaylord, and E.N. Glytsis*, Georgia Institute of Technology

2:25 "Electron inelastic mean free path and spatial resolution of BEEM." ***M.-L. Ke***, *C.C. Mathai, and R.H. Williams*, University of Wales College of Cardiff

2:40 "Effect of lattice mismatch on BEEM transport." ***T. Huang***, *H.D. Hallen, and R.A. Buhrman*, Cornell University

2:55 "The role of scattering in the metal film and at the interface in BEEM." ***R. Ludeke*** *and A. Bauer*, IBM Thomas J. Watson Research Center

3:20 **Poster Viewing**

4:30 **Summary Discussion:** "Important issues in BEEM." ***L.J. Schowalter***, Rensselaer Polytechnic Institute

5:30 Closing: ***Mark Stiles***, Program Chair, NIST

ELECTRON TRANSMISSION ACROSS INTERFACES AND SURFACES: AN OVERVIEW

Massimo V. Fischetti
IBM Research Division, Thomas J. Watson Research Center
P.O. Box 218, Yorktown Heights, NY 10598

Abstract

The problem of understanding how electron states behave at semiconductor interfaces and surfaces arises in a wide range of situations: quantized levels in quantum wells, transmission/reflections across heterojunctions, emission of photoexcited or hot carriers into metals and into vacuum. After a brief review of various theoretical approaches to tackle the state "matching" problem, several examples will be discussed of experiments whose analysis depends crucially on the model chosen. Among them, soft X-ray photoemission spectroscopy used to analyze high-energy electron transport in silicon and silicon dioxide, high-field vacuum emission from silicon dioxide, tunneling in the silicon-silicon dioxide system, and confined states and ballistic (vertical) transport in III-V III-V heterostructures. Emphasis will be given to a discussion of open problems, such as the issue of conservation of parallel momentum, of the role of surface/interface scattering and, more importantly, on the conservation of probability current across the discontinuity when using only envelope wavefunctions. Hopefully, my pessimistic conclusion—that a correct treatment is still beyond our reach—will be challenged by the audience.

BEEM STUDIES OF STRAIN-TUNED SEMICONDUCTOR INTERFACES*

S. J. Manion, L. D. Bell, W. J. Kaiser, A. M. Milliken, R. W. Fathauer, and M. H. Hecht

Center for Space Microelectronics Technology
Jet Propulsion Laboratory
California Institute of Technology
Pasadena, CA 91109

A new approach for the understanding of interfaces involves the tuning of interface properties by variation of such parameters as temperature, chemistry, and strain. The effects of these variables on interface electronic structure provides criteria for the evaluation of theories for interface formation. The precision of BEEM is an important aspect of the implementation of these studies.

BEEM provides an ideal method for characterizing the effects of strain on interface electronic structure. Heteroepitaxial growth by molecular-beam epitaxy was used to form strained $Si_{1-x}Ge_x$ layers on Si substrates. The degree of strain was controlled by varying the alloy fraction x. Effects of strain on the band structure of the SiGe will be described. For comparison, strained Si was also grown on a relaxed SiGe template, in order to separate effects due to interface chemistry from strain effects.

Efforts are also under way to perform BEEM measurements on strained Si substrates where the strain is induced by mechanical means. This method provides a way to continuously vary the applied strain while maintaining the same material system. Recent results will be discussed.

The variation of interface conditions by control of characteristics such as temperature and strain provides constraints for theories describing interface formation. Measurement of Fermi level movement and conduction band perturbations in metal/semiconductor systems where chemistry is held constant provides one way of evaluating basic Schottky barrier formation mechanisms. Objectives in this area of interface tuning will be described.

---

*Research supported by ONR and BMDO/IST

Transport Studies in Semiconductor Heterostructures Using BEEM*

T. Sajoto[1], J.J. O'Shea[2], S. Bhargava[1], D. Leonard[2], M.A. Chin[1], and V. Narayanamurti[1]
[1]Electrical and Computer Engineering Department
[2]Materials Department
University of California, Santa Barbara 93106

Ballistic Electron Emission Microscopy (BEEM) has been primarily used to study the charge transport across metal-semiconductor interfaces as well as the formation of the Schottky barrier[1]. We exploit BEEM to detect potential profiles of heterointerfaces buried *spatially beneath* the Schottky barrier.

We have used BEEM to measure the conduction band offsets in single barrier $Al_xGa_{1-x}As/GaAs$ structures and to study charge transport in $Al_xGa_{1-x}As/GaAs$ resonant tunneling structures grown by Molecular Beam Epitaxy. The single barrier structure consists of undoped GaAs with an $Al_xGa_{1-x}As$ barrier placed 100Å from the surface as shown in Figure 1. The resonant tunneling structure consists of a 17Å GaAs quantum well sandwiched between two 23Å $Al_{0.42}Ga_{0.58}As$ barriers placed 150Å from the surface as shown in Figure 2. A p-type (Be) δ-doped sheet is used in both cases to cancel the band bending, which allows us to obtain a direct measurement of the band offsets and energy levels.

BEEM spectra of the $Al_xGa_{1-x}As/GaAs$ single barrier structures with varying Al mole fractions were taken at 300K and 77K. Figure 3 shows 300K BEEM spectra for x=0.0, x=0.21, and x=0.42. The variation in the measured threshold voltage corresponds to the change in the conduction band offset as a function of Al mole fraction. The measured values of the conduction band offset at 300K and 77K for the single barrier structures are shown in Table 1.

Figure 4 shows a comparison of BEEM spectra for the x=0.42 single barrier structure and the resonant tunneling structure with x=0.42 $Al_xGa_{1-x}As$ barriers. Although both have an Al mole fraction of 0.42, the resonant tunneling structure has a *lower* threshold voltage. This indicates the existence of a bound state which was designed to be 0.25V above the bottom of the GaAs quantum well. In the inset to Figure 4, we have subtracted the 77K GaAs Schottky barrier height of 0.96V. The inset very clearly shows a change in slope at 0.24V, which we attribute to resonant tunneling. The additional structures in the BEEM spectra may be attributed to the higher energy AlGaAs barriers as well as higher energy GaAs satellite valleys.

The experimentally measured offsets as a function of Al mole fraction are consistent with the expected band-edge discontinuities[2]. Our results demonstrate that BEEM is a powerful characterization tool for measuring band-edge discontinuities and understanding the charge transport processes across spatially buried heterojunctions.

* This work was partially funded through a UC/MICRO grant with Surface/Interface Inc., and NSF grant #DMR-9313610.

[1] W.J. Kaiser and L.D. Bell, Phys. Rev. Lett. 60, 1406 (1988). We are grateful to Drs. W.J. Kaiser, M.H. Hecht, L.D. Bell, and S.J. Manion for many helpful suggestions and advice.
[2] S. Adachi, J. Appl. Phys. 58, R1 (1985).

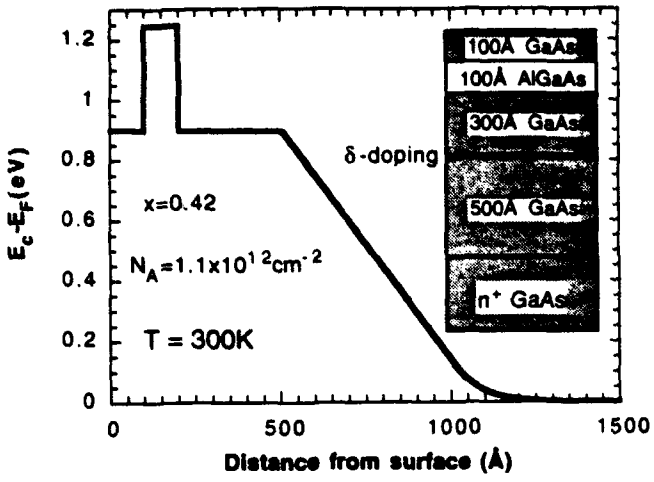

Figure 1. Sample structure and energy band diagram for AlGaAs/GaAs single barrier experiment.

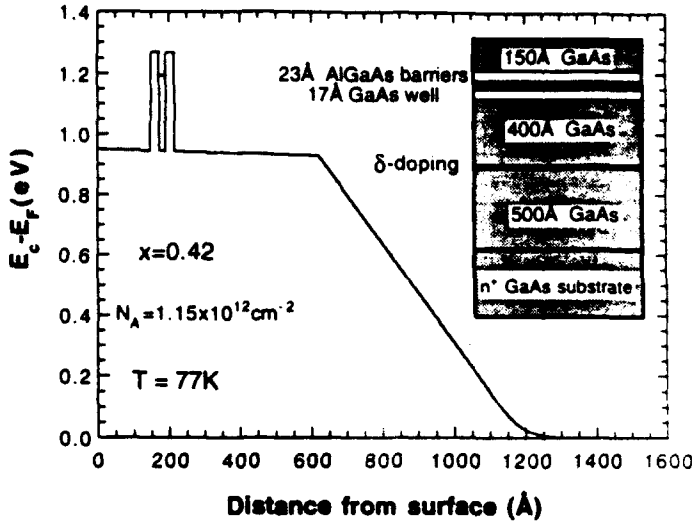

Figure 2. Sample structure and energy band diagram for the AlGaAs/GaAs resonant tunneling experiment.

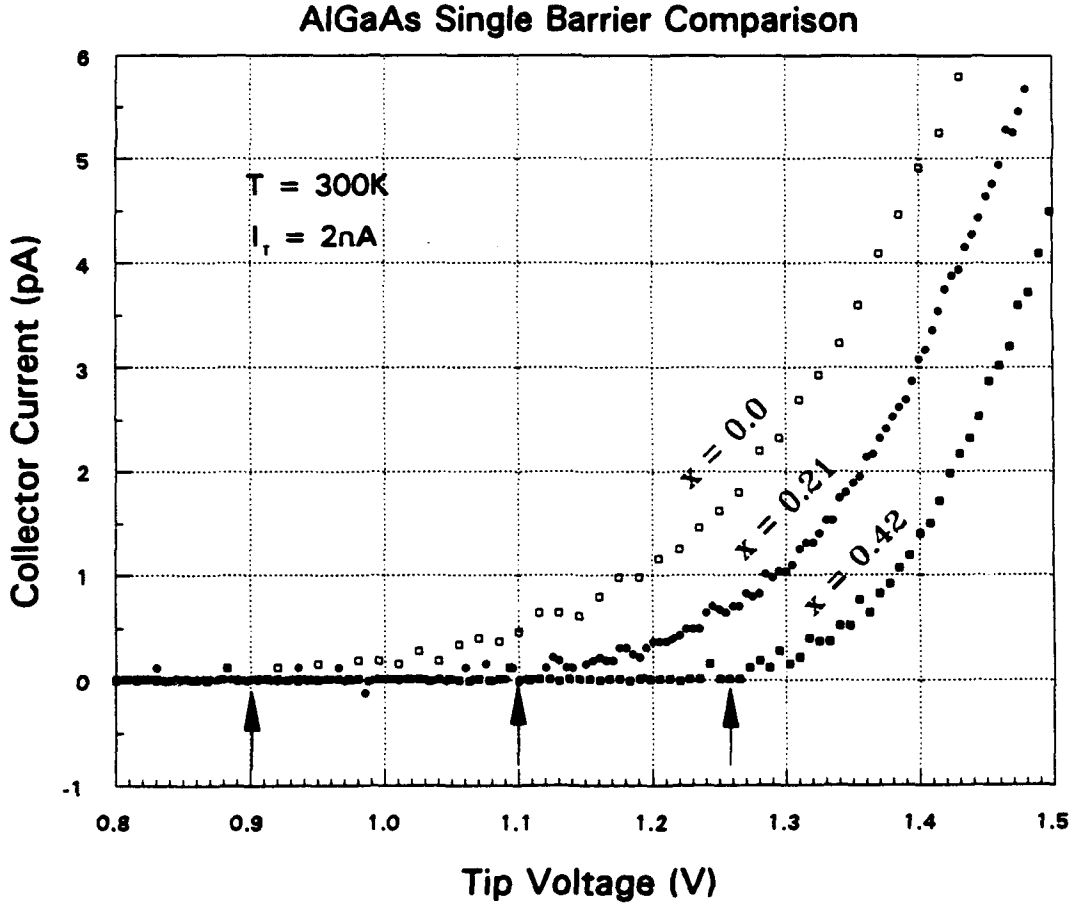

Figure 3. Variation of the BEEM threshold voltage as a function of the Al mole fraction.

T=300K		$E - E_{(x=0.0)}$
x = 0.0	0.90 eV	
x = 0.21	1.10 eV	0.20 eV
x = 0.42	1.26 eV	0.36 eV
Resonant Tunneling	1.10 eV	0.20 eV

T=77K		$E - E_{(x=0.0)}$
x = 0.0	0.96 eV	
x = 0.21	1.20 eV	0.24 eV
x = 0.42	1.33 eV	0.37 eV
Resonant Tunneling	1.20 eV	0.24 eV

Table 1. 300K and 77K turn-on voltages of the single barrier and resonant tunneling structures.

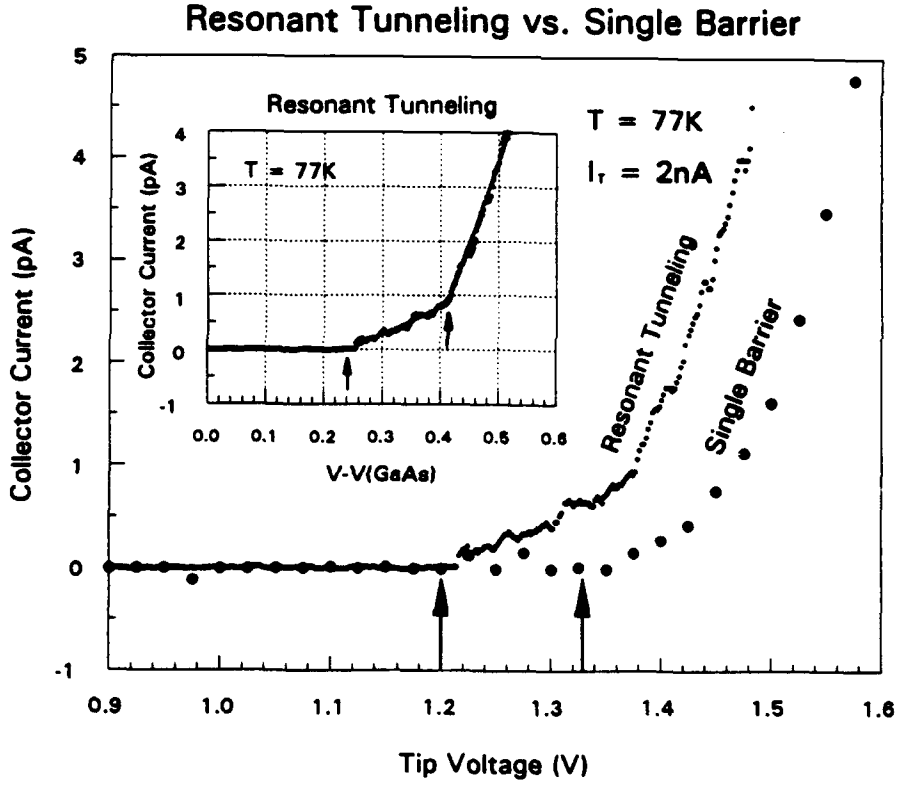

Figure 4. Comparison of the single barrier and resonant tunneling BEEM spectra. Note that the turn-on for the resonant tunneling structure is lower than that of the single barrier structure with the same x-value. The inset shows the same resonant tunneling BEEM spectrum with the 77K GaAs threshold subtracted.

Spectroscopic studies of quantum-wells and -wires using an STM

Lars Samuelson, Joakim Lindahl, Lars Montelius and Mats-Erik Pistol
Department of Solid State Physics/"nanometer structure" Consortium
Lund University, Box 118, S-221 00 LUND, Sweden

Introduction:

For the development of low-dimensional structures for use in physics and applications it is very important to have access to experimental techniques which are able to image and show existence and character of nano-structures as well as to develop experimental tools by which, not only ensembles of but also, individual low-dimensional structures can be investigated. We give in this study examples of spectrally resolved radiative recombination which is generated by local injection of carriers into the semiconductor structures from a scanning tunnelling microscope (STM) tip. We call this technique STL, scanning tunneling luminescence. We have found that it is of special interest to use as tip a degenerately doped semiconductor, since this mode of injection can allow an almost mono-energetic distribution in energy of the injected carriers. We specifically want to investigate ballistic injection of energetically tuned carriers injected from the STM-tip and to compare this with the less well controlled excitation obtained by cathodoluminescence (CL), with electrons having several keV in kinetic energy. These comparisons are made using samples containing quantum-wells as well as quantum-wires. We present data which show that the STM-induced excitation allows the generation of spectrally resolved luminescence from a single quantum-wire with good sensitivity and with quantum-wire luminescence having peak-widths of less than 20 meV.

Experimental approach:

For the study of STM induced luminescence we use a vibrationally damped STM hanging inside a cryostat equipped with windows for optical spectroscopy. The sample and the STM are thus either immersed in the cryogenic liquid (LN_2 or LHe) or in an exchange gas of He. In this case we use a camera lens to image the tip-sample region onto the entrance slit of a grating monochromator, which is equipped with a LN_2-cooled CCD-camera for parallell detection of spectra and for imaging of the sample-tip area during focussing of the experimental set-up. Figure 1 shows as an example the STM-tip (p-type GaP) together with the sample (InP wafer containing a few GaInAs QWs) imaged (a) during white light illumination of the tip-sample region, (b) using the emitted STL-light during tunnel injection.

Fig. 1 a b

The samples studied here were grown by MOVPE. In one case the sample contained a set of GaInAs QWs embedded in InP. The second type of sample to be presented here is grown on a corrugated GaAs substrate which is prepared using holographic interference and wet etching. On this substrate has been grown a GaAs/AlGaAs QW structure which forms a horizontal QW, a QW on the (111) side facets and where a quantum-well wire (QWR) is formed in the bottom of the grooves. Details of the fabrication of these sample structures can be found in original papers for the GaInAs/InP QWs by Seifert et al. and for the QWR-structure by Vermeire et al.

Experimental results and discussion:

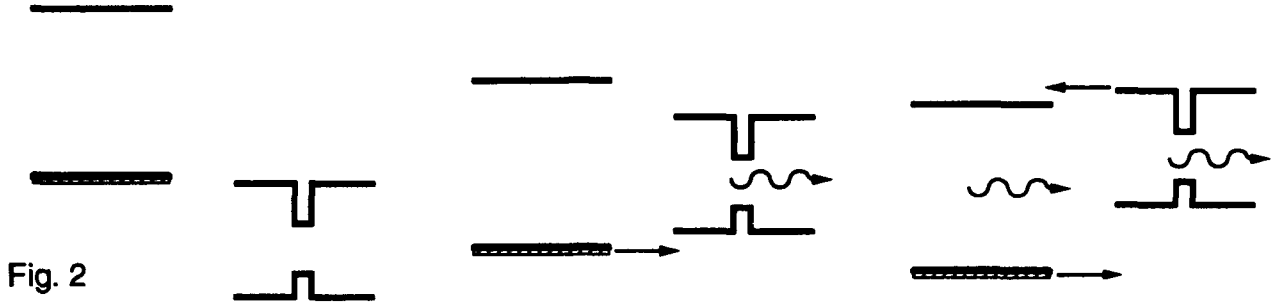

Fig. 2

In figure 2 we illustrate schematically the band-structure conditions for tunnel injection between a large band-gap, degenerately doped semiconducting tip and an n-doped sample containing QW structures. The main advantage with the use of such a degenerately doped, large band-gap semiconductor tip is that over a large range of biases the tunnel injection from such a tip occurs only from a very restricted range of energies, i.e. from the band-edge to the Fermi energy, which can be as narrow as a few meV. This is to be compared with tunneling from a metallic tip for which all allowed energies between the quasi Fermi energies of the tip and the studied sample will contribute to the current. We propose in this way that this tip-sample combination will allow finely tuned tunnel excitation spectroscopy to be made with the luminescence as a tagged probe to monitor the character of the tunneling as well as the scattering of ballistically injected carriers. We call this type of spectroscopy scanning tunnel induced luminescence excitation, STLE.

As an example of the phenomenological proposal for STLE in fig. 2 we show in fig. 3 a set of STL spectra obtained with a tip of degenerately p-doped GaP and an un-doped and weakly n-type epi-wafer of InP containing a set of very thin QWs positioned in the top 100 nm of the InP. The difference in bias between consecutive spectra is 125 meV. As seen in the spectra, a threshold for

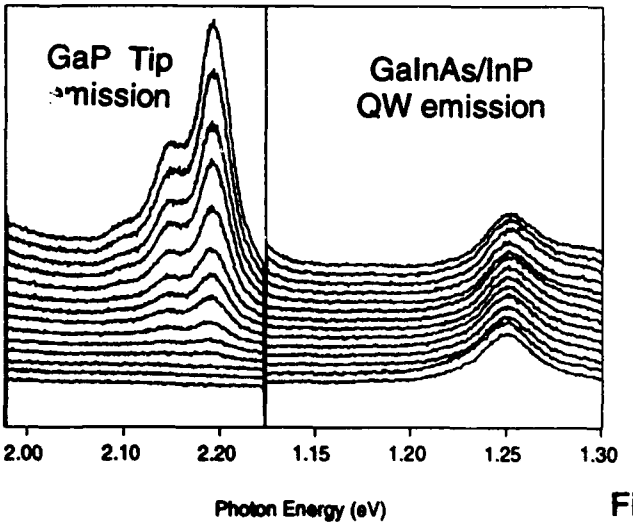

Fig. 3

excitation of different features is clearly visible: for lower bial levels only the excitation of the QW luminescence around 1.25 eV is observed, while for bias above the threshold one observes simultaneous excitation of the QW luminescence and of the characteristic donor-acceptor pair luminescence (at around 2.2 eV) from the GaP tip. These different biasing condition correspond to the conditions displayed in figure 2 (b) and (c). Hence, the spectrally resolved luminescence gives direct information of the character and directionality of the tip-sample injection conditions.

The last example of STL results that will be presented here are obtained from a study of a GaAs/AlGaAs quantum-well wire (QWR) sample grown on a corrugated substrate. Figure 4 shown in the insert a schematic of the sample geometry with the QWRs formed in the V-grooves and indicates also the two positions of the STM tip for which the luminescence was recorded. The top PL-spectrum is obtained during weak excitation of the tip-sample region using an un-focussed HeNe-laser. Based on studies of the same sample by CL (Gustafsson et al.), we can indentify the low energy peak at around 1.55 eV as originating from the QWRs and the higher energy peak around 1.6 eV as due to the QWs. The spectra in the lower portion of the figure are recorded (a) with the tip positioned just above one of the wires and in case (b) with the tip laterally moved a distance corresponding to half the spacing between the V-grooves. From the cleanliness of the spectra we can conclude that in case (a) we are able to selectively excite *one* QWR with negligible contributions from the surrounding QWs and in position (b) the lateral transport into the QWRs is very small. The current level required to record spectra from a single QWR is around 10 nA. From data like those in figure 4 we conclude that STL allows excitation of *individual* low-dimensional semiconductor structures like quantum-wires and quantum dots and that spectrally resolved data of high quality and narrow line-widths can be obtained.

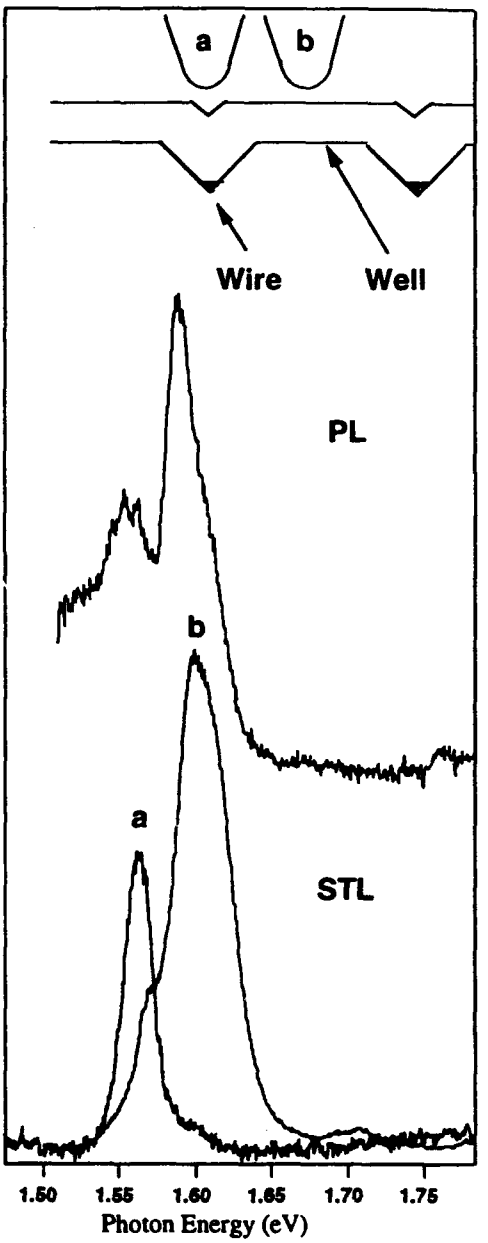

Fig. 4

References:

A Gustafsson, L Samuelson, J-O Malm, G Vermeire and P Demeester, APL **64** (1994)

L Samuelson, J Lindahl, L Montelius and M-E Pistol, Phys Scripta **T42**, 149 (1992)

W Seifert, J-O Fornell, L Ledebo, M-E Pistol and L Samuelson, APL **56**, 1128 (1990)

G Vermeire, Z Q Yu, F Vermaerke, L Buyens, P Van Daele and P Demeester, J. Crystal Growth **124**, 513 (1992)

BEEM in Pinholes of $NiSi_2$ Films on n-Si(111)-7×7: Determination of the Impact Ionization Quantum Yield in Si

A. Bauer

Institut für Experimentalphysik, Arnimallee 14, 14195 Berlin, Germany

R. Ludeke

IBM T.J. Watson Research Center, P.O. Box 218, Yorktown Heights, New York 10598

The large potential inherent in Ballistic Electron Emission Microscopy (BEEM) for studying hot electron transport in semiconductor devices is demonstrated in BEEM studies at $NiSi_2$/Si(111). BEEM spectra taken in pinholes of thin $NiSi_2$ films deposited on n-Si(111)-7×7 surfaces showed an extremely strong increase in collector current I_c, amounting to up to 210% of the tunneling current I_T at tip bias V_T = 10 V. This electron multiplication is assigned to impact ionization in the Si, i.e. the creation of electron-hole pairs in the depletion zone. By decomposing the spectra into a primary- and a secondary-electron component (the latter attributed to impact ionization), the quantum yield is given by the ratio of the two components. To our knowledge, this represents the most direct determination of the impact ionization quantum yield over a large energy range. Our results are in good agreement with recent theoretical calculations.

Sample preparation and BEEM experiments were performed in UHV. In order to reduce thermal noise in the collector current, very small $NiSi_2$ dots (0.25 mm in diameter) were grown on a clean n-Si(111)-7×7 surface, applying the template method [1]. The employed Si wafers were low n-type (P) doped (5 – 12 Ωcm). The deposited $NiSi_2$ films were mostly flat with terrace widths of typically 1000 Å. On thin $NiSi_2$ films (< 25 Å) pinholes of ≈ 100 – 1000 Å diameter were observed, wherein remnants of the Si(111)-7×7 surface reconstruction were found. Due to the high conductivity of the Si(111)-7×7 surface and the proximity of the surrounding metal film ($NiSi_2$), providing a sufficiently good conducting path to the metal-film contact, BEEM could also be performed in pinholes.

In Fig. 1, two BEEM spectra are shown, both taken at 22 Å $NiSi_2$/Si(111)-7×7. Spectrum B was taken on a $NiSi_2$ terrace, spectrum A in a pinhole of the $NiSi_2$ film. Representative 90 Å × 55 Å STM images of the areas where the spectra were recorded are shown in the inset of Fig. 1: On the $NiSi_2$ surface (lower STM image) the characteristic triangular Si islands are observed, while in the pinholes the surface is mostly unordered with only some remnants of the initial Si(111)-7×7 surface present (upper image). The observed differences between spectrum A and B - in spectrum B, I_c amounts to only 20% of that in spectrum A at high tip voltages and is in particular strongly reduced in the threshold region (V_T < 2 V) - cannot be accounted for by the difference in metal-film thickness ("zero thickness" for spectrum A) alone. However, there are significant differences in the transmission probability for electron transmission across the Schottky barrier expected, accounting for the observed effects. For the $NiSi_2$/Si(111) interface, relatively small transmission probabilities have been calculated [2]. In the pinholes, in contrast, the electrons tunnel from the tip directly into

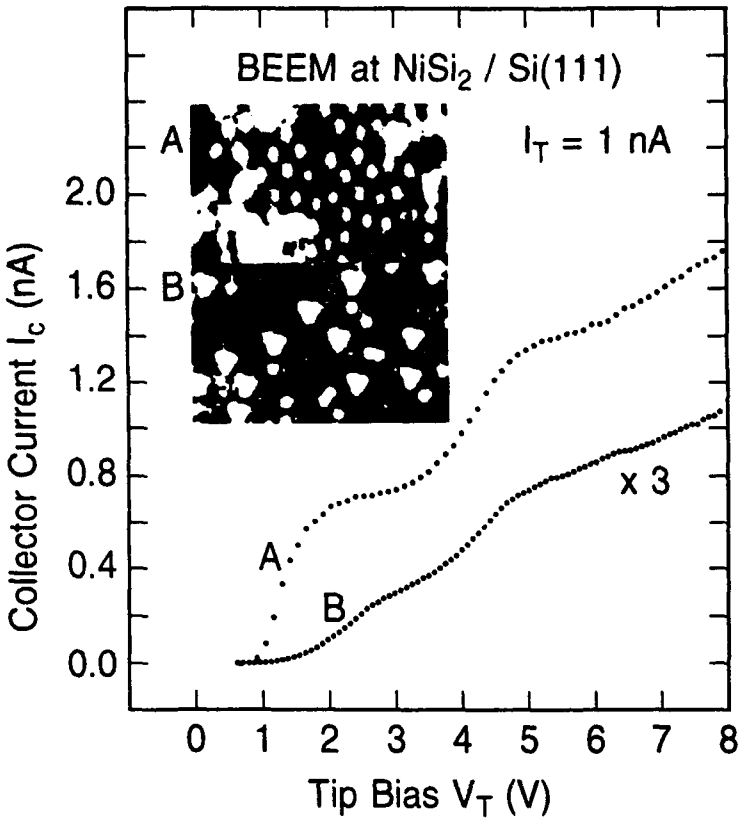

Fig.1

Si-surface states and surface resonances, the latter well coupling to propagating bulk states. In addition, due to a disordered surface in the pinholes responsible for non-conservation of transverse momentum, the electrons just above the Schottky barrier can be scattered into the conduction-band minima of the Si, accounting for the strong increase of I_c in the threshold region.

Since I_c exeeds I_T in the pinholes where the electrons tunnel directly into the Si, the second threshold in the spectra can unambigiously be assigned to the onset of impact ionization. In Fig. 2(a), spectrum A (curve 1) is decomposed into a primary- (curve 2) and a secondary-electron component (curve 3). The primary component was simulated using the model of Ludeke et al. [3]. It is basically a 5/2-power law in the threshold region that transforms smoothly to a constant value at higher tip voltages. The parameter of the model were freely adjusted, and since I_c saturates before impact ionization gives a significant contribution the simulation is facilitated. In this way, a saturation current as high as 72% of I_T was deduced, directly corresponding to the transmission probability. The impact ionization quantum yield, γ, is given by the ratio of secondary electrons (curve 3) to primary electrons (curve 2). In Fig. 2(b), γ is plotted as a function of the kinetic energy in Si, $E_{kin} = qV_T - V_0$, where V_0 is the Schottky-barrier height, which was found to be the same as for the surrounding $NiSi_2$ film: $V_0 = 0.79$ eV (see inset of Fig. 2a). As is clearly seen, at $E_{kin} \approx 5$ eV there is a further threshold when γ exceeds unity, i.e. double impact ionization sets in.

The experimental findings are in excellent agreement with a rather simple theory by Alig et al. [4] with only one adjustable parameter, A, characterizing the strength of impact ionization relative to electron-phonon scattering, and also with Monte-Carlo calculations by Cartier et al. [5] based on a complex theory that takes the actual bandstructure of Si into account. The two curves according to Alig's theory correspond to $A = 5.2\ (eV)^3$, the previously determined value [4], (solid line), and

$A = 7.5\ (eV)^3$, an adjusted value to give the best fit. Consistent with both theories is a soft threshold for impact ionization at $E_{th} = \frac{3}{2} E_g \cong 1.7$ eV, where E_g is the band gap of the semiconductor.

In the same way as presented here for Si, the impact ionization quantum yield for other semiconductors can be determined from BEEM spectra taken on very thin metal films on the respective semiconductor substrate, where scattering effects in the metal layer are still negligible. In order to avoid a variation in E_{kin} due to the changing electric potential in the depletion zone of the semiconductor, low doped substrates ($< 10^{15}$ cm^{-3}) have to be used so that the dethermilization processes (impact ionization and electron-phonon scattering) occur within a region of small potential variation.

This work was supported by the Deutsche Forschungsgemeinschaft, project Pr289/2-1.

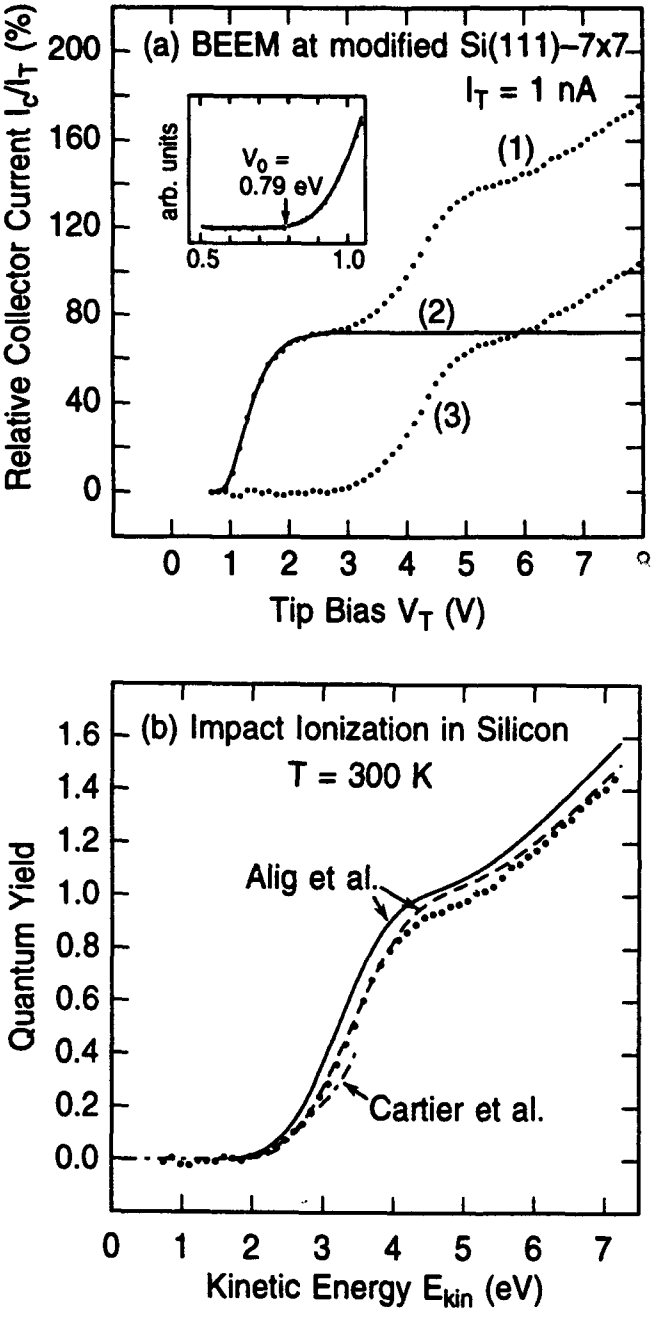

Fig. 2

[1] R.T. Tung, J.M. Gibson, and J.M. Poate, Phys. Rev. Lett. **50**, 429 (1983).
[2] M.D. Stiles and D.R. Hamann, Phys. Rev. Lett. **66**, 3179 (1991).
A. Bauer, R. Ludeke, and M.D. Stiles, to be published.
[3] R. Ludeke, M. Prietsch, and A. Samsavar, J. Vac. Sci. Technol. B **9**, 2342 (1991).
[4] R.C. Alig, S. Bloom, and C.W. Struck, Phys. Rev. B **22**, 5565 (1980).
[5] E. Cartier, M.V. Fischetti, I.A. Eklund, and F.R. McFeely, Appl. Phys. Lett. **62**, 3339 (1993).

Low-temperature UHV ballistic-electron-emission microscopy of epitaxial $CoSi_2$/Si(111)

H. von Känel, E. Y. Lee, and H. Sirringhaus
Laboratorium für Festkörperphysik, ETH Hönggerberg, CH-8093 Zürich

Among the spectroscopic tools capable of providing high spatial resolution, ballistic-electron-emission microscopy (BEEM) and spectroscopy (BEES) are probably the most outstanding [1]. In its most common application, i.e. the study of potential barriers at buried interfaces, the spatial resolution of BEEM is limited only by the rate at which the potential barriers to carrier transport may vary on a lateral scale. Most BEEM/BEES studies have so far been dedicated to the metal/semiconductor interface, where the potential profile due to Schottky barrier inhomogenieties is of major concern.

In the present study of epitaxial $CoSi_2$ thin films on Si(111) we shall not so much emphasize on the energetics of the interface itself, which has already been investigated in some detail [2]. The main focus will rather be to correlate as fully as possible the surface topography and spectroscopy, as determined by scanning tunneling microscopy (STM) and by BEEM.

Our experiments have been performed with a low-temperature UHV-STM designed for in-situ BEEM/BEES studies of 3-inch samples prepared by molecular beam epitaxy (MBE). The STM has proved to yield atomic resolution both at room temperature and at 77 K.

For the present study $CoSi_2$ films with thicknesses between 20 and 70Å were grown on n^+-Si(111) substrates after the MBE growth of a 1μm thick undoped Si buffer layer. All films were prepared with the elastic stress due to the misfit at least partly relaxed. As shown elsewhere [3], this leads to a hexagonal network of interfacial misfit dislocations inducing a surface deformation which is measurable by STM. In Fig.1a is shown an example of a topographic STM image acquired on a 25Å thick film. The contrast due to the misfit dislocations gives rise to the network of faint lines crossing the monolayer surface steps virtually undisturbed. The corresponding BEEM image exhibits much stronger contrast variations as can be seen in Fig.1b. The BEEM current is considerably enhanced at both the surface steps and at the buried dislocations. The scattering leading to the enhanced BEEM current appears to be confined mainly to the dislocation core rather than to the elastic strain field surrounding the dislocation line. This follows from comparison of cross-sectional profiles across dislocations. Typical profiles taken from Fig.1 (dashed line) are shown in Fig.2. The topographic cross-section (filled symbols) yields a Lorentzian profile with a half-width given by the film thickness [3], whereas the corresponding profile of the BEEM current is much narrower (open symbols).

Apart from those due to scattering at steps and dislocations, the BEEM image of Fig.1b exhibits planar contrast variations of another kind. STM topographs taken at atomic resolution indicate that they are at least partly due to changes of the surface structure which may affect the tunneling current distribution. Strained $CoSi_2$/Si(111) films have previously been shown to

exhibit a 2x1 surface reconstruction related to that of cleaved Si(111) [4]. Even though the strain of the films considered here is partly relaxed, the difference in thermal expansion of Si and $CoSi_2$ results in sufficient strain for large areas to reconstruct at 77 K.

Electron scattering at buried dislocations leads also to small but discernible features in BEES. Spatially resolved BEES at 77 K is possible due to the sufficiently small thermal drift rate of the microscope. The two spectra in Fig.3 were taken with a constant tunneling current of 2nA right on top (open circles) and next to the dislocation (filled circles). The onset of the BEEM current is at Vs=-0.66±0.03V, independent of the location. In accordance with the BEEM image of Fig.1b, the collector current is enhanced on the dislocation line by as much as 20% at -2V. There are subtle differences in the corresponding derivative spectra (insert in Fig.3), which appear, however, to depend also on the kind of dislocation considered and possibly on the film thickness and surface structure.

[1] W. J. Kaiser, and L. D. Bell, Phys. Rev. Lett. 60, 1406 (1988)

[2] W. J. Kaiser, M. H. Hecht, R. W. Fathauer, L. D. Bell, E. Y. Lee, and L. C. Davis, Phys. Rev. B 44, 6546 (1991)

[3] R. Stalder, H. Sirringhaus, N. Onda, and H. von Känel, Appl. Phys. Lett. 59, 1960 (1991)

[4] R. Stalder, H. Sirringhaus, N. Onda, and H. von Känel, Surf. Sci. 258, 153 (1991)

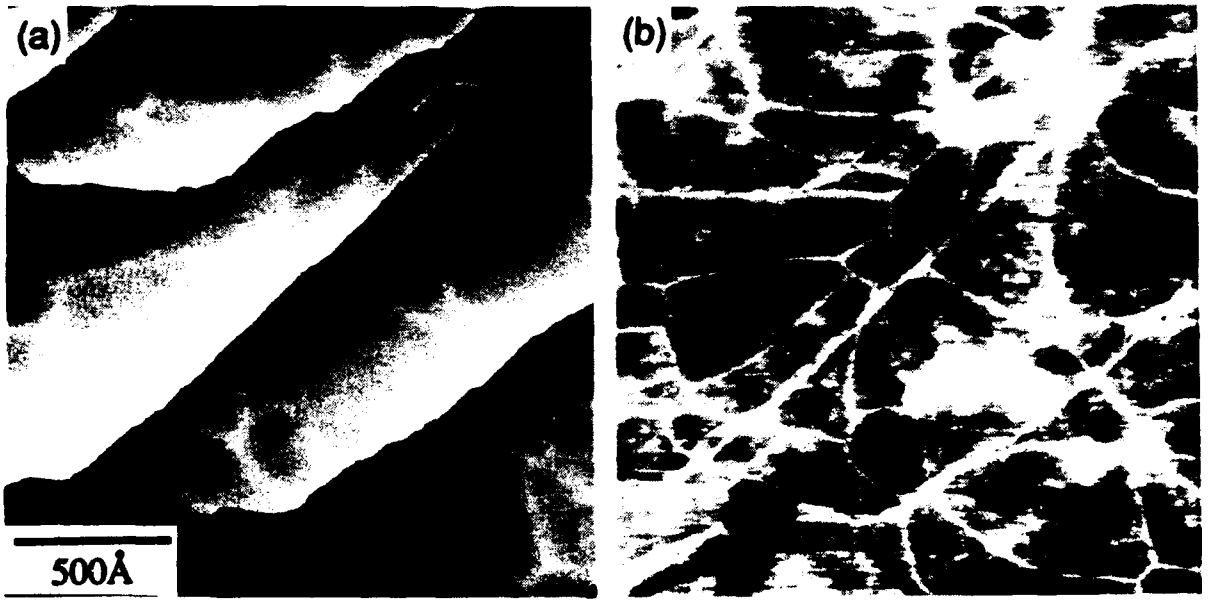

Fig.1: STM topograph (a) and corresponding BEEM image (b) obtained at 77 K on a 25Å $CoSi_2$/Si(111) film. The current scale in (b) ranges from ~0 (black) to 100pA (white) (stabilization tip bias voltage V_t= -2V, tunneling current I_t= 5nA). The dashed line indicates the location of the profiles shown in Fig.2.

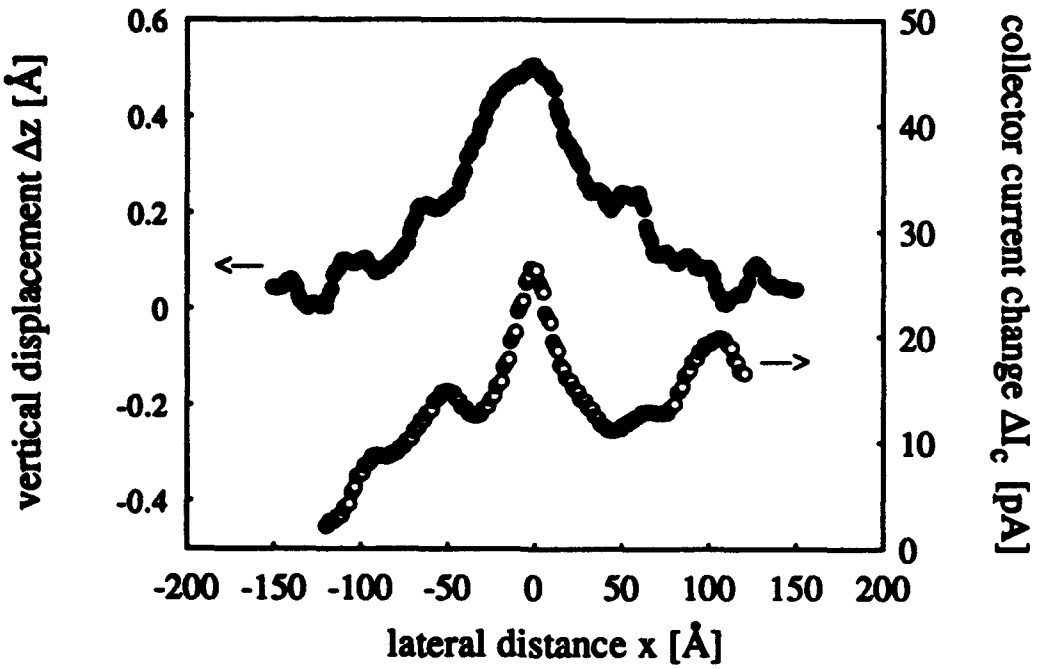

Fig.2: Cross-sectional profiles taken from the topography (filled symbols) and the BEEM image (open symbols) of Fig.1, respectively.

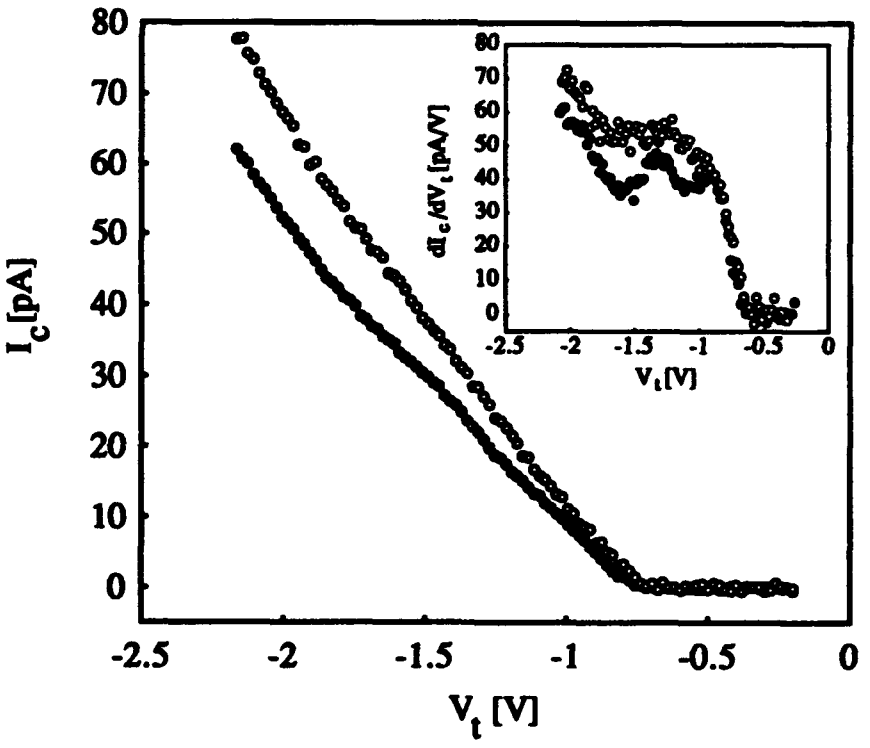

Fig.3: BEES spectra measured right on top of a dislocation line (open circles) and next to it (filled circles). Each of them is an average over ~50 single spectra. The tunneling current was set to 2nA and the tip stabilization voltage to -2V. In the insert the calculated derivative spectra are shown.

Interfacial Barrier Studies of Epitaxial CoGa on n-type (100)GaAs with Ballistic-electron-emission Microscopy

Liming Tsau, T. C. Kuo, and K. L. Wang
Device Research Laboratory, Department of Electrical Engineering
University of California, Los Angeles
Los Angeles, CA 90024-1600

Abstract

Ballistic-electron-emission microscopy (BEEM) has been used to investigate the Schottky barrier heights (SBH) at CoGa/GaAs interfaces. The CoGa layers of different epitaxial phases ((100), (110) and a mixture of both) grown on n-type (100)GaAs substrates have been studied. The growth techniques by molecular-beam-epitaxy (MBE) have been described elsewhere [2]. After the MBE growth, BEEM measurements were performed by using an ambient scanning tunneling microscope (STM).

A typical I-V curve for the (110)CoGa/(100)GaAs interfaces is shown in Fig. 1. The turn-on voltage was found to be about 1.24 eV, which is about 0.28 eV higher than that for the (100)CoGa/GaAs interfaces as reported in Ref[1]. This agrees with the result obtained from conventional I-V and C-V measurements which shows that the (110)CoGa/(100)GaAs interface has a higher SBH than the (100)CoGa/(100)GaAs interface [3, 4]. In addition, the spatial variation was also studied. While the (100)CoGa/(100)GaAs interface gives a turn-on voltage of high spatial uniformity [1], the turn-on voltage of the (110)CoGa/(100)GaAs interfaces ranges from ~1.05 V to ~1.3 V, as can be seen in Fig. 2. This may be a result of the lattice mismatch at the (110)CoGa/(100)GaAs interface [2]. The spatial variation of the turn-on voltages for the mix-phase CoGa/(100)GaAs interfaces was found to be even higher. Fig. 3 gives a distribution of the turn-on voltages for the mix-phase case.

References

[1] Liming Tsau, T. C. Kuo, and K. L. Wang. *Appl. Phys. Lett.*, 63, 1062, 1993.

[2] T. C. Kuo, T. W. Kang and K. L. Wang. *J. Crys. Growth*, 111, 996, 1991.

[3] T. C. Kuo, R. Arghavani, and K. L. Wang. *J. Appl. Phys.*, 73, 1191, 1992.

[4] T. C. Kuo, K. L. Wang, R. Arghavani, T. George, and T. L. Lin. *J. Vac. Sci. Technol.*, B10, 1923, 1992.

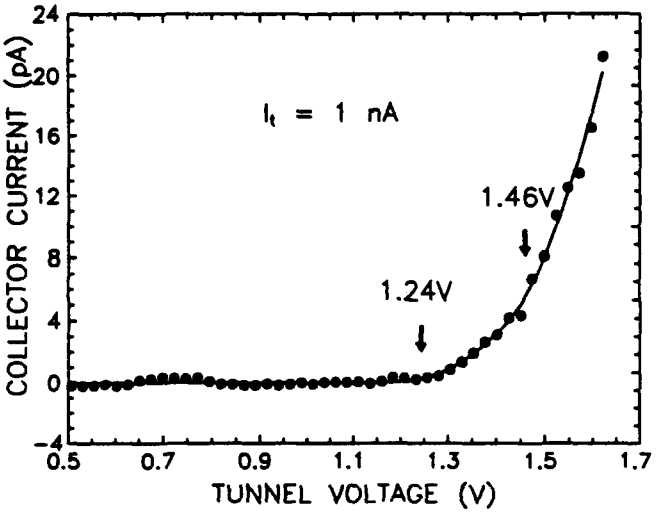

Figure 1 : BEEM spectrum of 35 Å (110)CoGa/n-type (100)GaAs for a tunnel current of 1 nA. The collector current I_C and its fit are shown by the dots and the solid line, respectively. The two threshold voltages, as indicated by the arrows, were extracted by using the Bell and Kaiser model and assuming the ballistic electrons were injected into the X-valley and L-valley only.

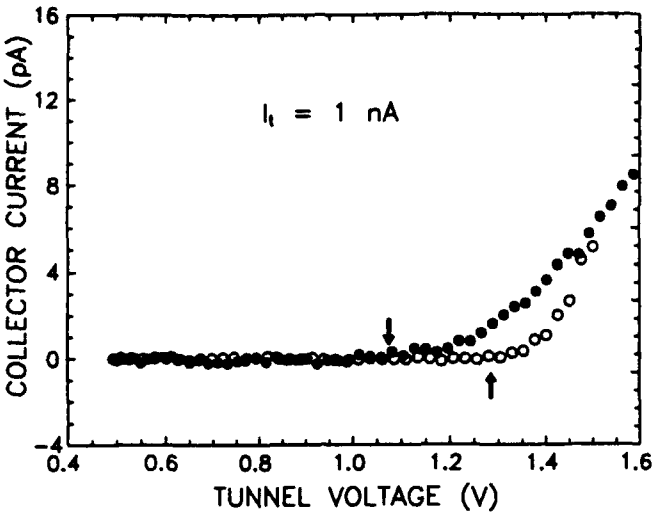

Figure 2 : BEEM spectra of 35 Å (110)CoGa/n-type (100)GaAs at two different locations for a tunnel current of 1 nA, as shown by the open circles and the filled circles. The turn-on voltage for the filled circles is about 0.2 eV lower than that for the open circles, as indicated by the arrows.

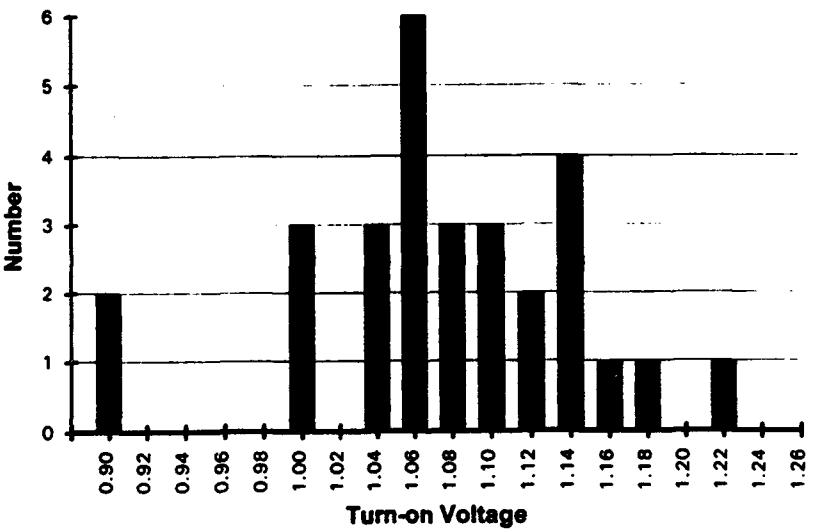

Figure 3 : Histogram of the number of times each turn-on voltage was observed for the 35 Å mix-phase CoGa/n-type (100)GaAs interface. This distribution was based on 28 measurements at different locations on the same sample.

BEEM on Au/Si(111)7×7 and Au/CaF_2/Si(111)7×7

M.T. Cuberes,[a] A. Bauer, H.J. Wen, M. Prietsch, and G. Kaindl

Institut für Experimentalphysik, Freie Universität Berlin,
Arnimallee 14, D-14195 Berlin-Dahlem, Germany

The capability of BEEM to probe the electronic properties of MIS (metal-insulator-semiconductor) structures as well as to investigate phenomena related to hot-electron transport through thin insulating films has been experimentally tested for the Au/CaF_2/Si(111)7×7 interface. BEEM on both Au/Si and Au/CaF_2/Si demonstrate that the CaF_2 electronic band structure restricts the electron transport through the Au/Si interface to an about 3 eV narrow energy window, as expected according to density-of-state calculations for bulk CaF_2.

The experiments were performed at room temperature completely under UHV conditions (1×10^{-10} mbar). *n*-type Si(111) wafers (phosphorus doped with ρ = 10 - 20 Ωcm) were used as substrates, and annealed to 900°C to prepare clean Si(111)7×7 surfaces. Epitaxial CaF_2 layers were deposited at a substrate temperature of 750°C, and 40 Å thick Au dots with 1 mm diameter were evaporated with the sample at room temperature, both at rates around 3 Å min^{-1}. The use of highly doped *n*-type Si clamps (ρ = 0.01 Ωcm) for good ohmic back-contacts as well as the low pressure during sample preparation (< 2×10^{-9} mbar) proved to be essential for detecting a BEEM current.

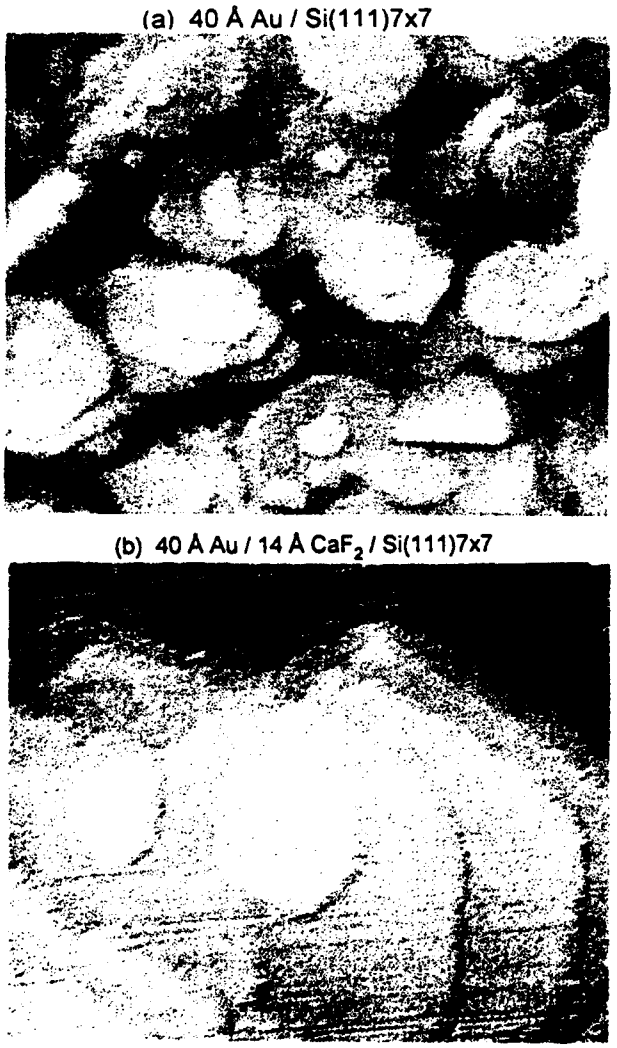

Figure 1

Fig. 1 shows 500 Å × 400 Å STM images of the surface topography (a) without and (b) with a 14 Å thick CaF_2 intralayer. The Au/Si interface is characterized by round terraces of ≈ 25 Å diameter on top of larger terraces, also circular in shape with ≈ 100 Å diameter. Up to four different levels can be distinguished, with step heights varying from 2 to 3 Å. The Au/CaF_2/Si interface is also characterized by ≈ 2.5 Å heigh terraces stacked in several stages, but in this case larger and with well-defined hexagonal shapes.

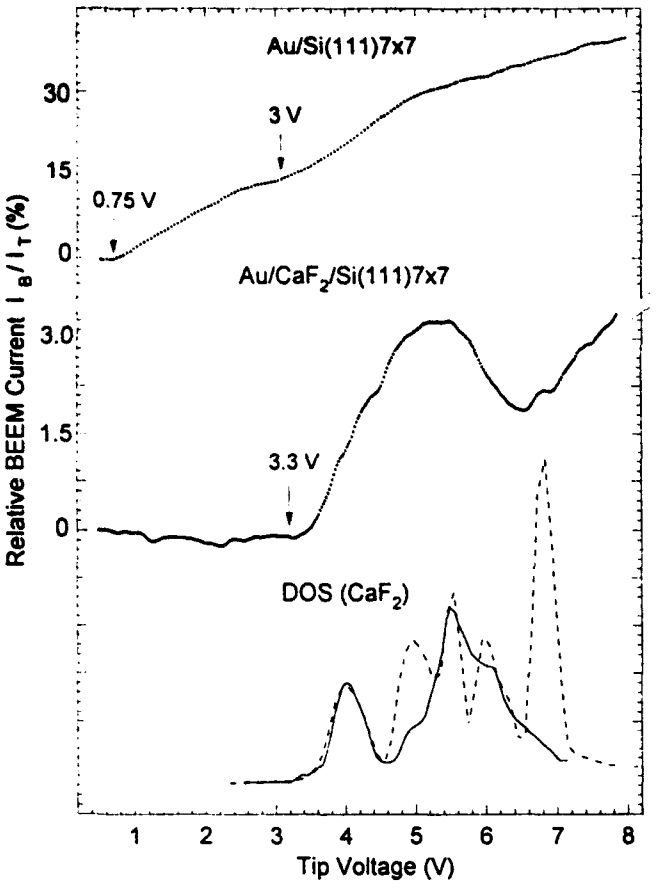

Figure 2

Representative BEEM spectra taken of these interfaces up to tip voltages of 8 V are shown in Fig. 2. Spectrum (a) was taken on the Au/Si(111) interface. From a detailed measurement in the threshold region, a Schottky-barrier height of 0.75 ± 0.03 eV is derived [1]. The additional threshold at about 3 V is related to the onset of impact ionization in Si.

Spectrum (b) was obtained by averaging 14 selected spectra measured on the Au/CaF_2/Si interface. It shows a threshold at about 3.3 eV, and the relative BEEM current I_B/I_T at V_T = 8 eV is about one order of magnitude smaller than for Au/Si. Assuming that the onset of the BEEM current is determined by the CaF_2 conduction-band minumum (CBM) and taking into account the image-force potential lowering in the intralayer, estimated to 0.5 eV at the center of the intralayer, a value of about 3.8 eV is obtained for the position of the CBM in the CaF_2 intralayer relative to E_F.

The strong decrease of the BEEM current at voltages around 6 V can be related to the band structure of the CaF_2 film. The spectra at the bottom of the figure represent the theoretical shape of the density of states (DOS) for bulk CaF_2, as calculated by different approaches (dashed [2], continous [3]). An inspection of the figure shows that the CaF_2 DOS determines the energy window for the electron transport through the intralayer rather well. The almost linear increase of the BEEM current for voltages ≥ 6.6 V is attributed to the contribution of inelastically scattered electrons in the Au overlayer and impact ionization in Si, as also observed in Fig. 2(a) [1].

The BEEM spectrum is reproducing some spectral features of the DOS of bulk CaF_2 and can – in principle – be used to test different theoretical calculations. However, the interpretation of these results is not so straightforward because of several reasons: (i) Even in case of an isotropic distribution of electrons incident on the CaF_2 layer, only information on the DOS weighted in (111) direction is obtained in a transport measurement, (ii) electron-wave confinement inside the 14 Å thick epitaxial CaF_2 film is expected to result in the formation of standing waves, quantisized in energy for each propagating direction of the hot electrons, (iii) the electronic

Figure 3

structure of such a thin intralayer can differ from that of bulk CaF_2 due to strong interface effects, (iv) the energy width of the tunneling current as well as inelastic scattering of the hot electrons in the Au film has to be taken into account, (v) the nature of the states - localized or itinerant - may have an impact on their ability for transport, and (vi) the transmission coefficient throught the Au/CaF_2 and the CaF_2/Si interfaces and the Si band structure can also affect the spectral shape. In this way, both the dispersion of the CaF_2 electronic band structure and the total density of states have to be considered for the interpretation of the BEEM spectra.

In contrast with previous reports [4], increasing the tip voltage up to 8 V did not alter the ballistic transmissivity neither at Au/Si nor at $Au/CaF_2/Si$. However, the collection of BEEM spectra up to these high voltages slightly distorted the surface topography. This is demonstrated in Fig. 3, where an 800 Å × 800 Å STM image of the $Au/CaF_2/Si(111)$ interface is shown together with the grid of the positions of the BEEM spectra taken during the scan. Scanning in a line-by-line mode started in the lower left corner, and each BEEM spectrum was acquired when the tip reached the respective grid position. It is easily observed that each BEEM spectrum, taken at tip voltages up to 8 V, results in the formation of about 3 Å high protrusions up to distances of 50 Å from the point where the spectrum was taken, indicating slight modifications of the metal surface.

This work was supported by the Deutsche Forschungsgemeinschaft, project Pr289/2-1. One of the authors, M.T.C., gratefully acknowledges financial support from the Consejo Superior de Investigaciones Cientificas, Spain.

a) permanent address: Instituto de Ciencias de Materiales, CSIC, Serrano 144, E-28006 Madrid, Spain.

[1] M.T. Cuberes, A. Bauer, H.J. Wen, D. Vandré, M. Prietsch, and G. Kaindl, J. Vac. Sci. Technol. B, submitted (1993).
[2] F. Gan, Y.-N. Xu, M.-Z. Huang, W.Y. Ching, and J.G. Harrison, Phys. Rev. B **45**, 8248 (1992).
[3] C. Arcangeli, S. Ossicini and O. Bisi, Surf. Sci. **269/270**, 743 (1992).
[4] A. Fernandez, H.D. Hallen, T. Huang, R.A. Buhrman, and J. Silcox, Appl. Phys. Lett. **57**, 2826 (1990).

Temperature Dependence of Schottky Barriers as Probed by Ballistic Electron Emission Microscopy*

S. Bhargava[1], J.J. O'Shea[2], T. Sajoto[1], D. Leonard[2], M.A. Chin[1] and V. Narayanamurti[1]
[1]Electrical and Computer Engineering Department
[2]Materials Department
University of California, Santa Barbara 93106

W.J. Kaiser, M.H. Hecht, L.D. Bell, and S.J. Manion
Jet Propulsion Laboratories, Pasadena, California 91109

C.E. Bryson, III and M. Ackeret
Surface/Interface Inc., Mountain View, California 94041

The majority of BEEM work to date has been performed on systems with Schottky barrier heights which can be conveniently measured at room temperature. The study of low Schottky barrier height systems requires low temperature measurements for reasonable diode sizes. We have developed a variable temperature BEEM apparatus which operates in air for $300K \leq T \leq 77K$. Since our BEEM experiments were performed in air, we have selected a surface preparation which produces robust samples that do not degrade when exposed to the ambient.

We have used Ballistic Electron Emission Microscopy (BEEM) to study Au on n-type and p-type Si wafers as well as Au on GaAs layers grown by Molecular Beam Epitaxy (MBE) on n-type and p-type GaAs substrates. GaAs samples were prepared in a 1:5::NH_4OH:deionized water (DI) solution for 90sec and immediately rinsed in DI for 1min, then blown dry with nitrogen gas. Schottky diodes were fabricated by thermal evaporation of 100Å Au in 1mm diameter dots at a typical background pressure of $3x10^{-7}$Torr.

Figure 1 shows the 77K BEEM spectra for Au/n-Si and Au/p-Si which have Schottky barrier heights of 0.82V and 0.35V, respectively. These values are consistent with previously reported BEEM results [1] and the expected Si energy gap of 1.17eV [2].

We have measured both Au/n-GaAs and Au/p-GaAs samples as shown in Figure 2 down to 77K. Figure 3 shows the first low temperature measurements of Au/n-GaAs which indicate an increase in the Schottky barrier height from 0.90V at 300K to 0.96V at 77K. We have also measured Au/p-GaAs at 77K and obtained a Schottky barrier height of 0.54V. The sum of the barrier heights is in good agreement with the expected 77K GaAs energy gap as shown in Figure 4 [3].

We have also performed BEEM experiments utilizing an electrochemically-etched, heavily-doped semiconductor tip. A preliminary BEEM spectra obtained with a Si tip for a Au/n-Si sample has a similar threshold to data taken with a Au tip, as shown in Figure 5. We expect the semiconductor tip to enhance the energy resolution of the BEEM technique and further experiments are in progress.

* This work was funded through a CalTech President's Award and a UC/MICRO grant with Surface/Interface Inc.

[1] L.D. Bell, M.H. Hecht, W.J. Kaiser, and L.C. Davis, Phys. Rev. Lett. 64, 2679 (1990).
[2] Landolt-Börnstein Vol. 22, Springer-Verlag (1987).
[3] J.D. Blakemore, J. Appl. Phys. 53, R123 (1982).

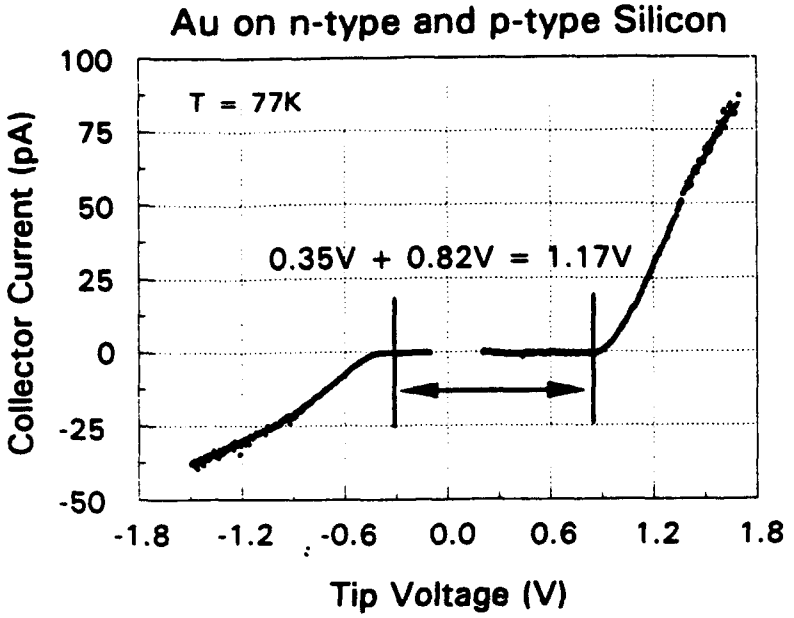

Figure 1: BEEM spectra for Au on n-type and p-type Si measured at 77K. The Schottky barrier heights add up to the expected energy gap of Si of 1.17eV.

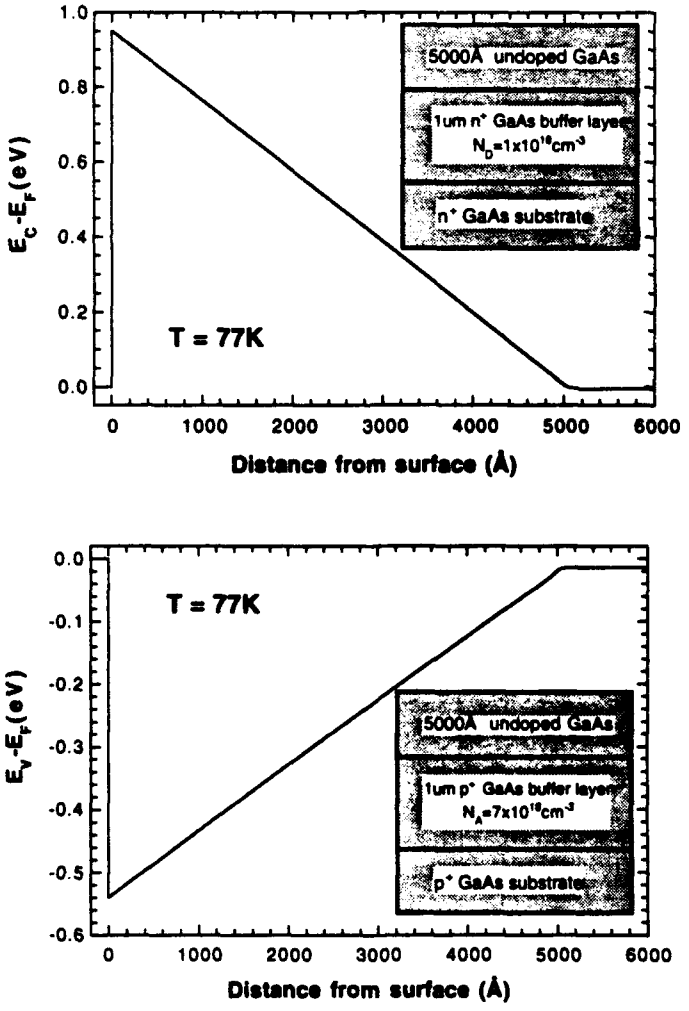

Figure 2: Calculated energy band diagrams at 77K for n-type and p-type MBE-grown GaAs structures. The background doping in the undoped layers was assumed to be $N_A=1x10^{14}cm^{-3}$. The n-type and p-type Schottky barriers are taken to be 0.95eV and 0.54eV, respectively.

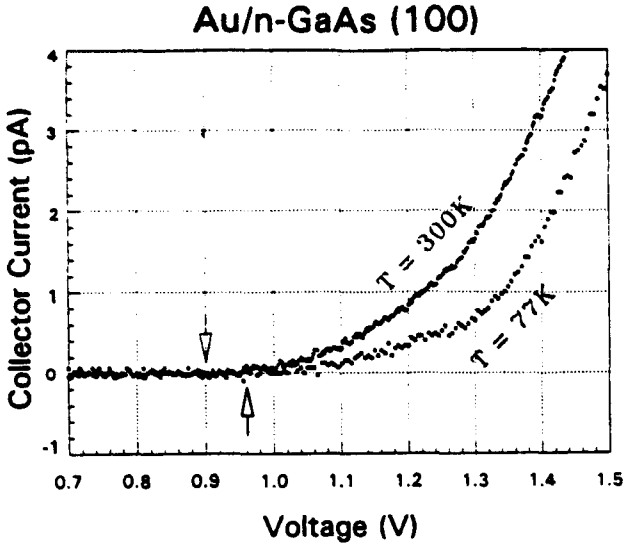

Figure 3: Comparison of n-type GaAs BEEM spectra taken at room temperature and 77K.

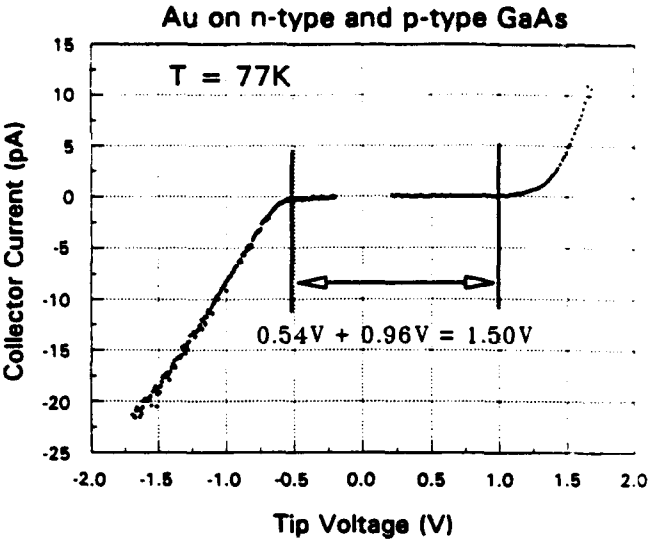

Figure 4: BEEM spectra for Au on n-type and p-type GaAs taken at 77K. The sum of the Schottky barrier heights is in agreement with the expected GaAs band-gap of 1.51eV.

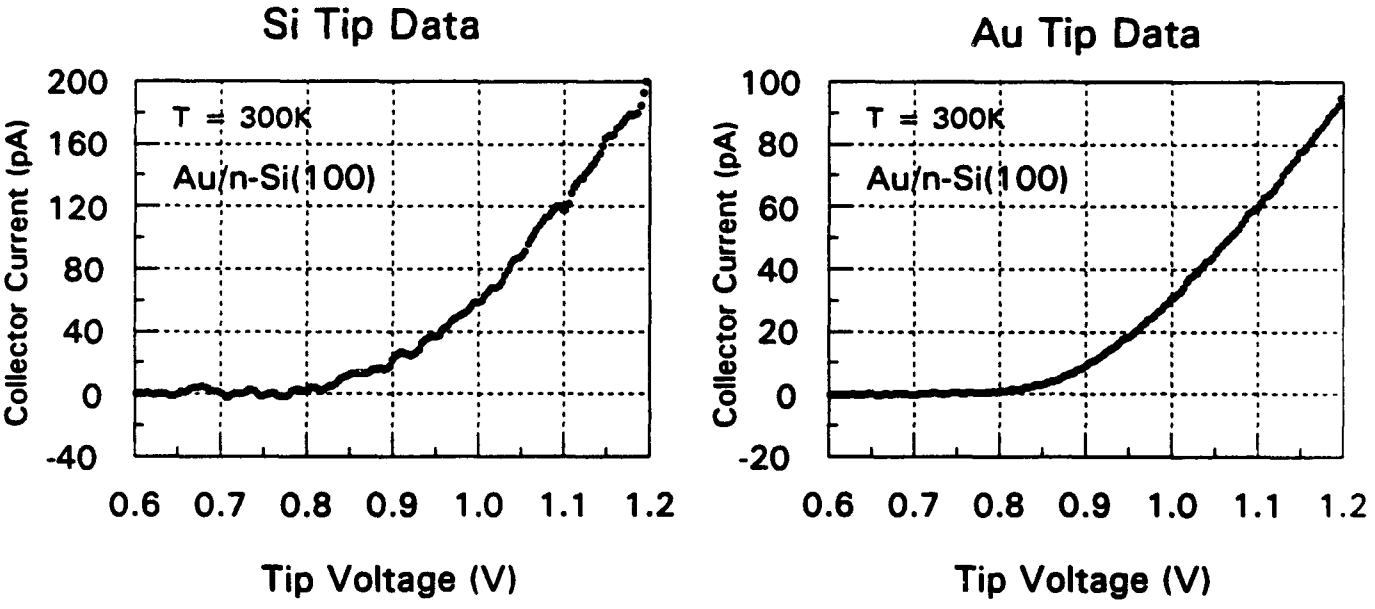

Figure 5: Comparison of BEEM spectra of Au/n-Si measured with a Si tip and BEEM spectra taken with a Au tip which show a similar turn-on voltage.

Nanoscopic Barrier Height Distributions at Metal/Semiconductor Interfaces and Observation of Critical Lengths

Brent A. Morgan, Ken M. Ring, Wayne Bi,
Charles W. Tu, and Karen L. Kavanagh
University of California San Diego, La Jolla, CA 92093-0407

A. Alec Talin, Tue Ngo, and R. Stanley Williams
University of California Los Angeles, Los Angeles, CA 90024-2569

Spatial variations in the Schottky barrier height have been of ongoing concern in the literature as the cause of discrepancies between barrier heights measured by current-voltage and by capacitance-voltage methods[1-5]. The existence of such barrier height distributions necessarily means that diodes smaller than a certain critical area will show a significant variation in observed barrier height. This has important implications for manufacture of uniform arrays of contacts (eg. photo diode arrays) and for small MESFET gate contacts.

We have measured BEEM barrier heights at random locations and on line scans in the following metal semiconductor systems: Au/Si, Au/GaAs, Au/$In_xGa_{1-x}P$ and PtSi/Si. The resulting barrier height distributions analyzed with the parallel conduction model[4] gave good agreement with barrier heights determined by IV and CV methods when image force lowering and thermionic field emission were considered.

To determine critical lengths the RMS deviation of the barrier height from the global average as a function of length was determined from line scan data. Critical lengths were found to scale with the Debye length of the substrate. Surface and interface morphologies as imaged with STM or cross-sectional TEM had length scales significantly different from the critical length determined from BEEM analysis.

1. J.L. Freeouf, T.N. Jackson, S.E. Laux, and J. M. Woodall, Appl. Phys, Lett., **40**, 634 (1982).
2. J.H. Werner and H.H Güttler, J. Appl. Phys., **69**, 1522 (1991).
3. R.T Tung, Phys. Rev. B., **45**, 13209 (1992).
4. S. Chang, A. Raisanen, L. J. Brillson, J.L. Shaw, P.D. Kirchner, G.D. Pettit, and J.M. Woodall, J. Vac Sci. Tech. B, **10**, 1932 (1992).
5. I. Ohdomari and K.N. Tu, J. Appl. Phys., **51**, 3735 (1980).

Acknowledgements: This work was supported in part by a contract from the SDIO monitored by the ONR, a California MICRO grant with Hughes Aircraft Co., NSF DMR-PYI and DMR-9202692, and the Powell Foundation.

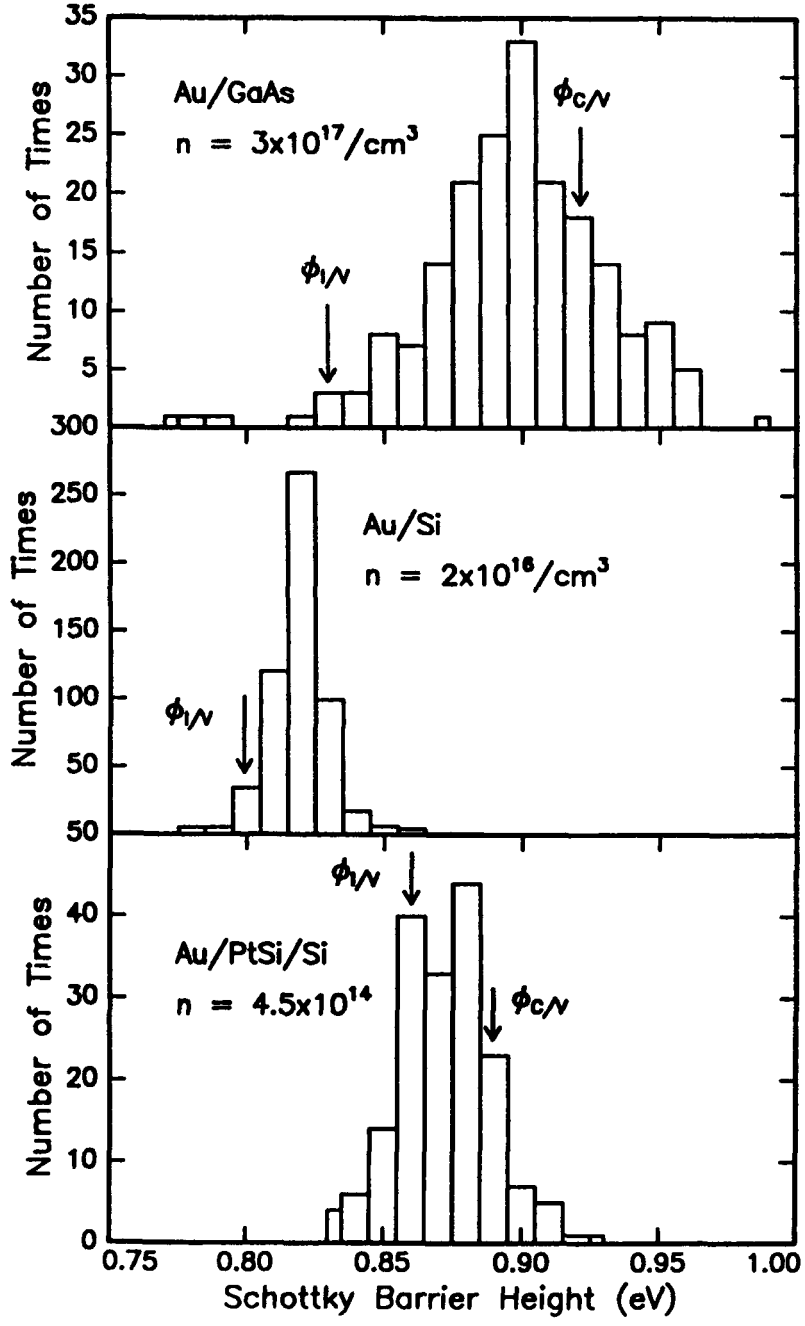
Au/GaAs
n = 3x10^17/cm^3
Au/Si
n = 2x10^16/cm^3
Au/PtSi/Si
n = 4.5x10^14
Number of Times
Schottky Barrier Height (eV)

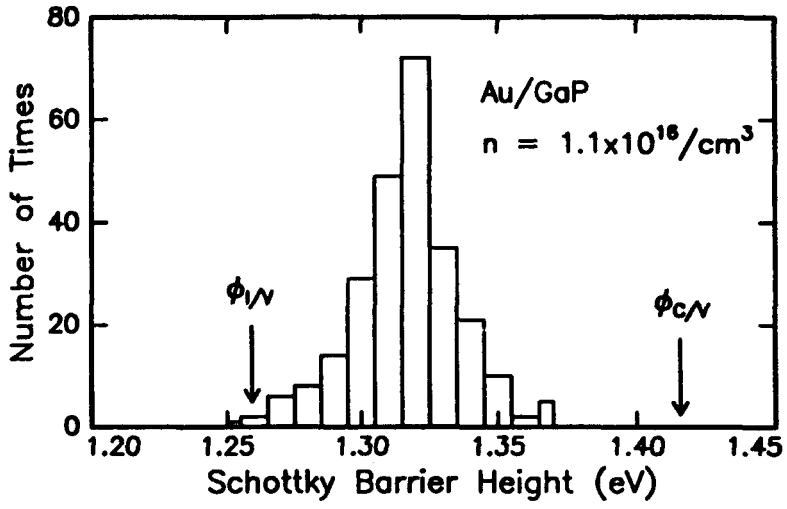
Au/GaP
n = 1.1x10^16/cm^3
Number of Times
Schottky Barrier Height (eV)

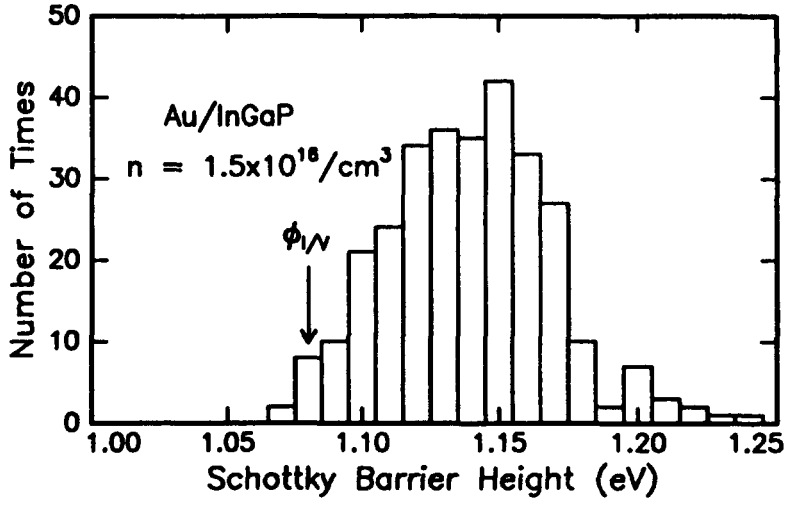
Au/InGaP
n = 1.5x10^16/cm^3
Number of Times
Schottky Barrier Height (eV)

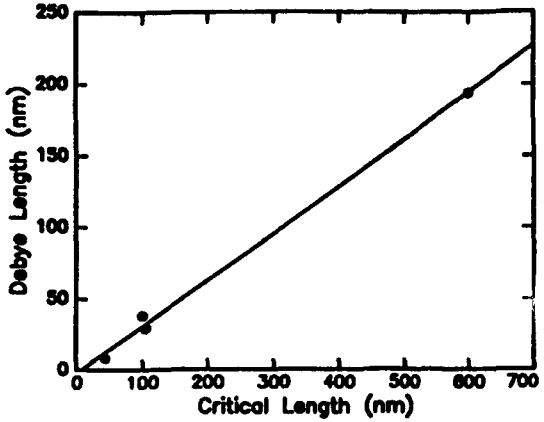
Debye Length (nm)
Critical Length (nm)
0
50
100
150
200
250
0
100
200
300
400
500
600
700

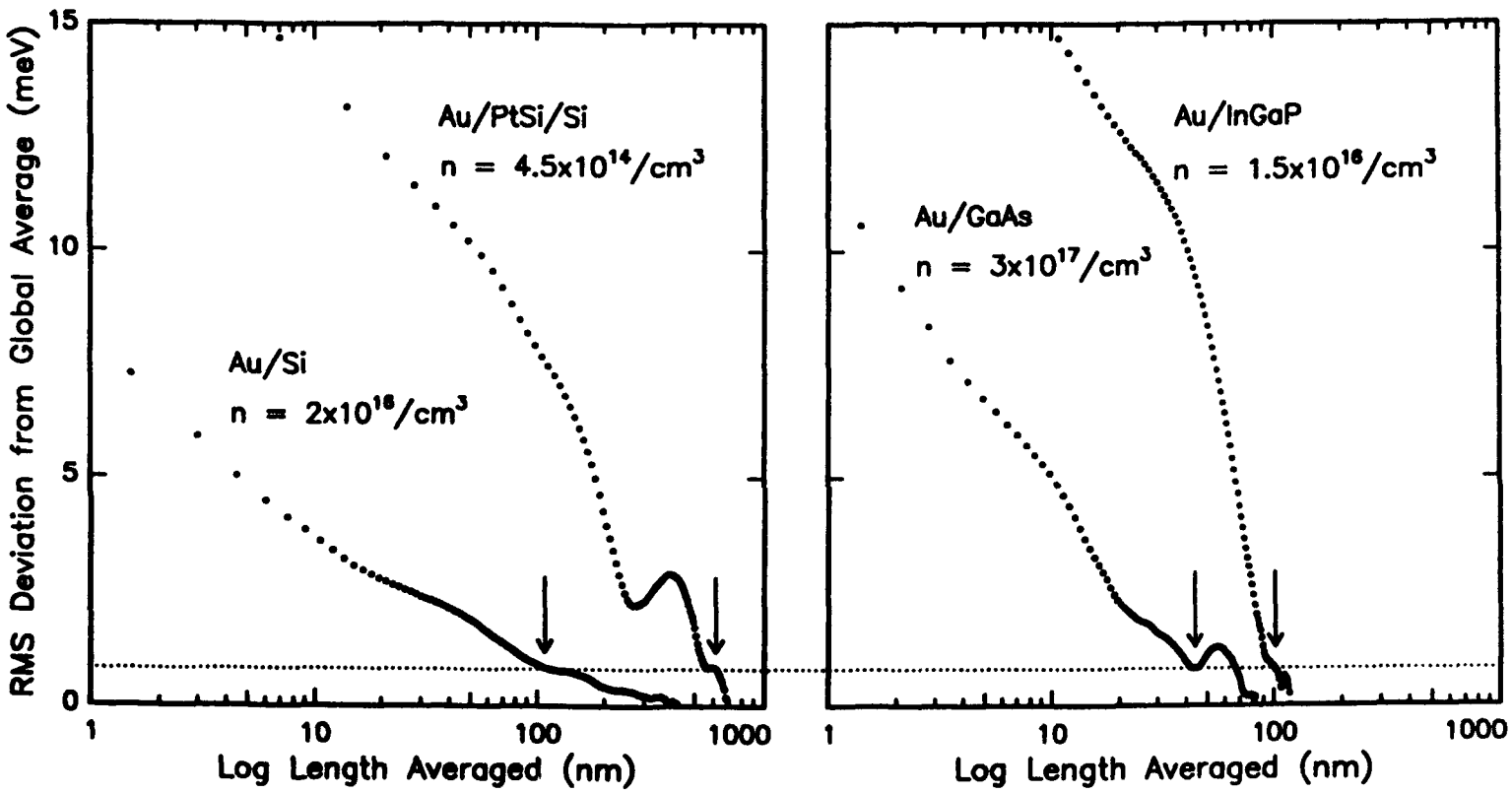
RMS Deviation from Global Average (meV)
Au/PtSi/Si
n = 4.5x10^14/cm^3
Au/Si
n = 2x10^18/cm^3
Au/InGaP
n = 1.5x10^16/cm^3
Au/GaAs
n = 3x10^17/cm^3
Log Length Averaged (nm)
Log Length Averaged (nm)
0
5
10
15
1
10
100
1000

BEEM Studies of Reverse-Biased Schottky Diodes

Angela Davies and Harold G. Craighead
Applied and Engineering Physics Department
Cornell University, Ithaca, New York, 14850

We have used ballistic electron emission microscopy (BEEM) to study Au/Si Schottky diodes under reverse bias conditions. By applying a bias across the diode, the conduction band minimum (CBM) profile in the semiconductor is controllably modified. Varying the potential profile in this way has allowed us to study the effects of the image potential lowering and hot-electron scattering processes in silicon.

Figure 1 shows an energy band diagram of the experiment. Many collector current spectra were taken at different locations on the sample for several reverse bias values. The spectra were analyzed using the 3-step phase-space model[1] with the addition of quantum mechanical transmission for a step-potential at the interface. For each I_C-V_t, we also calculated a threshold variation parameter. This quantity is the average deviation from the fit at each data point in the threshold region, normalized to the expected deviation. We use this parameter to measure the quality of the fits to the data. A mean threshold variation of zero indicates that the data on average is well described by this model. An example of a typical collector current spectrum is shown in figure 2a, as well as the phase-space model fit. Also shown in the figure is the definition of the threshold variation parameter.

We observe interesting behavior in the mean threshold variation dependence on reverse bias (see figure 2b.) This parameter, for the unbiased diode, is on average negative and approaches zero as the reverse bias is increased. This indicates there is a voltage dependence to the transport which is not included in the phase-space model; moreover, this voltage dependence is sensitive to the shape of the CBM profile in the semiconductor. This will result in discrepancies in the interpretation of the parameters extracted using this model.

The dependence of the mean barrier height on reverse-bias is shown in figure 3a. The barrier height is reduced on average by ~10mV over this reverse bias range. Also shown in the figure is the expected dependence due to the image potential lowering[2]. We believe the observed deviation is the result of the phase-space analysis as was mentioned above.

Over this reverse bias range, we find that the mean scaling factor increases by ~10% (see figure 3b.) This increase is likely due to a reduction in the percentage of back scattered electrons, which are electrons that cross the potential maximum in the semiconductor but are subsequently scattered back into the base. We are currently doing Monte Carlo simulations to verify this field strength dependence.

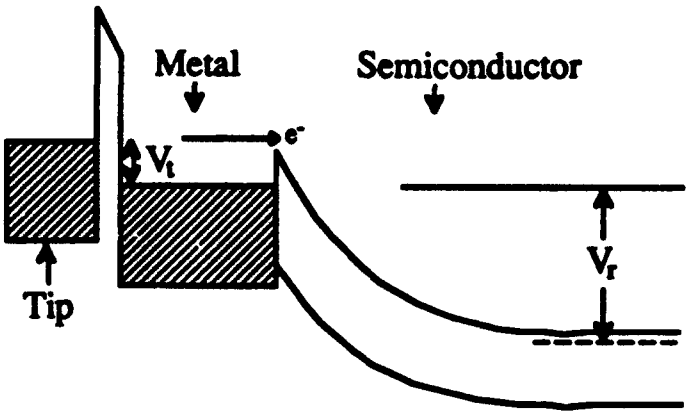

Figure 1. Energy band diagram of BEEM with device under reverse bias. V_r is the metal-semiconductor reverse bias and V_t is the tip-metal voltage.

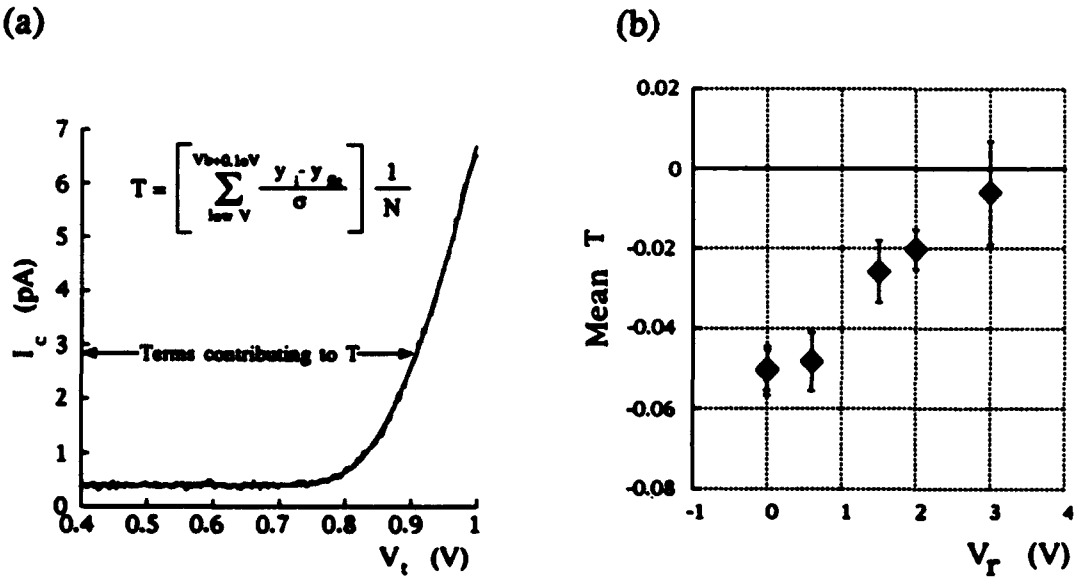

Figure 2. (a) Example of a collector current spectrum and the phase-space model fit. Also shown is the definition of the threshold variation parameter where N is the number of terms in the sum and σ is the standard deviation of the collector current below threshold. (b) Mean threshold variation dependence on reverse bias.

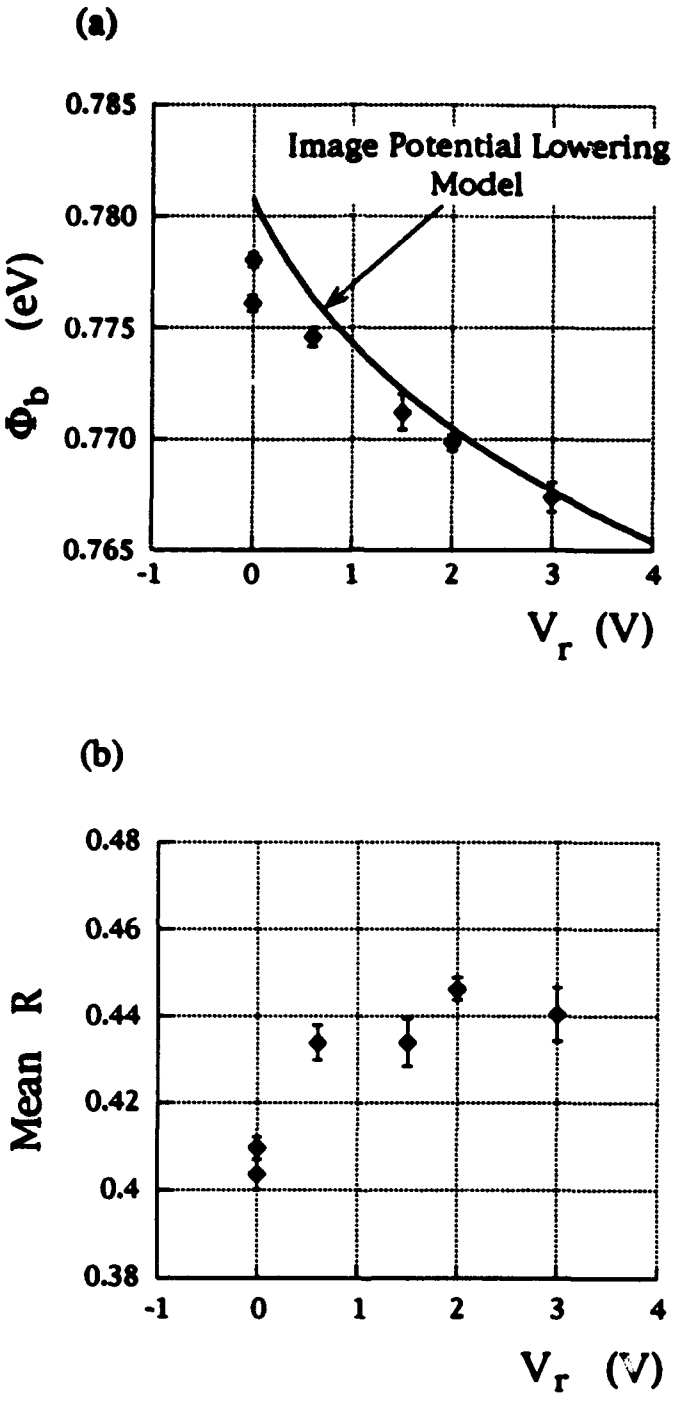

Figure 3. (a) Mean barrier heights determined from phase-space analysis. The solid curve is the expected barrier height dependence due to image potential lowering. (b) Mean scaling factor dependence on reverse bias.

[1] L. D. Bell and W. J. Kaiser, Phys. Rev. Lett. 61, 2368 (1988)

[2] S. M. Sze, *Physics of Semiconductor Devices*, 2nd ed. (Wiley, New York, 1981), chapter 5.

Ballistic Models Applied to Low-Temperature BEEM Measurements of Au/Si Interfaces

Daniel K. Guthrie, Gregory N. Henderson, Lee E. Harrell,
Phillip N. First, Thomas K. Gaylord, and Elias N. Glytsis
School of Electrical and Computer Engineering, School of Physics, and Microelectronics Research Center
Georgia Institute of Technology, Atlanta, Georgia 30332

The ballistic description of BEEM spectra for Schottky interfaces proposed by Bell and Kaiser (BK) [1] has been utilized for several years in the characterization of sub-surface interface electronic properties. The majority of the reported results deal with room-temperature measurements in which thermal noise and drift prohibit high resolution data from being obtained. Using a recently developed low-temperature STM, high resolution, high signal-to-noise ratio data near threshold have been obtained. The ballistic model [2] has been extended to include electron transmission into off-axis ellipses for both (100) and (111) BEEM spectra. This model also includes the energy dependence of the transmittance into both the zone-centered and the off-axis ellipses. 77K experimental data have been compared to the model to discern whether or not the energy dependence of the transmittance can be resolved. In addition, the dependence of the spectra upon the electron momentum distribution was investigated by varying the distribution from the usual planar tunneling case to a completely isotropic angular distribution. The distribution was broadened by assuming that a fraction of the electrons scattered isotropically as described by

$$F(\theta) = \ell f_1(\theta) + (1 - \ell) f_2(\theta) \tag{1}$$

where $f_1(\theta)$ is the planar tunneling distribution, $f_2(\theta)$ = constant is an isotropic distribution, and ℓ is the unscattered fraction of electrons.

The results of these comparison for Si(100) data with an isotropic distribution are shown in Fig. 1. The inset shows an expanded threshold region which extends approximately $100\,mV$ above threshold. The extended BK model, which assumes $T = 1$ and includes the outer (100) energy ellipses falls below the data while the QT model fits the data remarkably well. A plot of mean squared error vs. the fit range is shown in Fig. 1b. The error associated with the BK model rises linearly with fit range, while the QT model remains flat until approximately 200 mV above threshold. The QT model gives a significantly better fit for all distributions from $\ell = 1$ to 0. Preliminary Si(111) experimental data have been used to investigate the amount of scattering that must be included in the model to reproduce the experimentally observed magnitudes and shape. It has been found that moderate amounts of scattering ($\ell = 0.4$ as shown in Fig. 2) will produce good fits to the observed magnitude and shape of the spectra as shown in Fig. 3.

[1] L. D. Bell and W. J. Kaiser, *Phys. Rev. Lett.* **61**, 2368 (1988).

[2] G. N. Henderson, *et al.*, *Phys. Rev. Lett.* **71**, 2999 (1993).

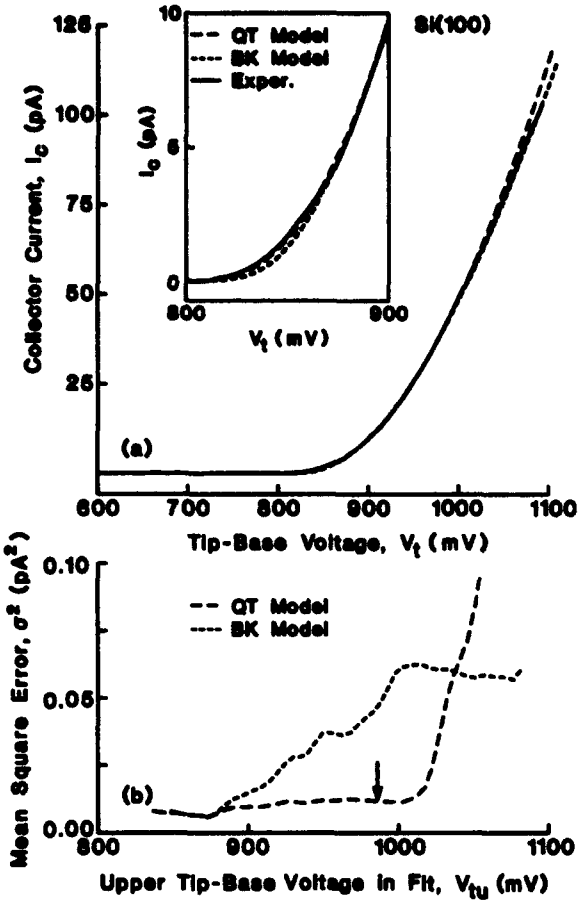

Fig. 1: (a) Comparison of the least square fits of 77K Au/Si(100) BEEM spectrum to the models which ignore (BK) and include (QT) the quantum transmittance of the metal semiconductor interface considering an isotropic distribution ($\ell = 0.0$). (b) Mean square error for the BK and QT models vs. the fit range, from $742mV$ to V_{tu}. The arrow indicates V_{tu} for the fits shown in (a).

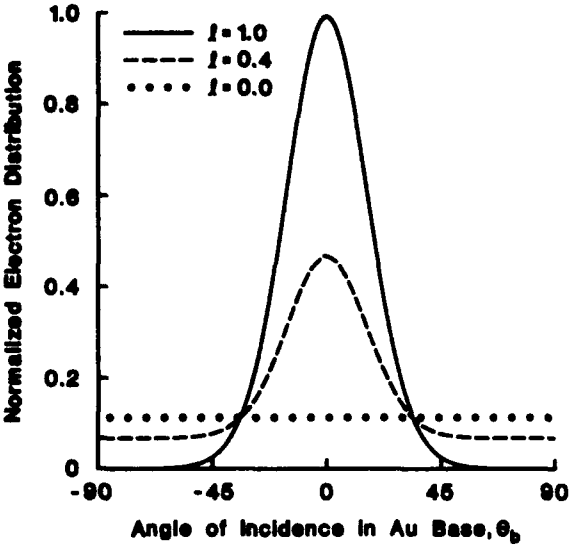

Fig. 2: Electron momentum distribution from planar tunneling ($\ell = 1.0$) to isotropic ($\ell = 0.0$). Moderate amounts of scattering ($\ell = 0.4$ as shown in Fig. 3) will produce good fits to the observed magnitude and shape of (111) spectra.

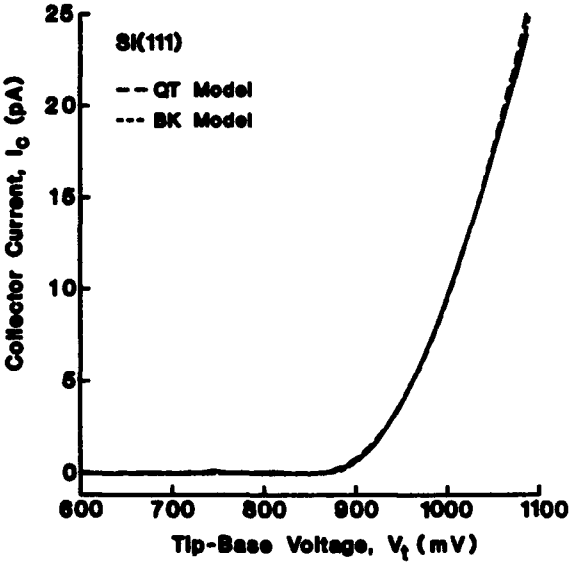

Fig. 3: 77K Si(111) data fit using a broadened electron momentum distribution of $\ell = 0.4$ as shown in Fig. 2.

ELECTRON INELASTIC MEAN FREE PATH AND SPATIAL RESOLUTION OF BEEM

Mao-Long Ke, C. C. Mathai and R. H. Williams
Department of Physics and Astronomy
University of Wales College of Cardiff
Cardiff, CF2, 3YB, UK

ABSTRACT

The Inelastic mean free path (IMFP) of an electron excited just above the Fermi surface has been calculated for gold by statistical approach. Both exchange effect and d-band contribution have been incorporated in the calculation. The results have been used in our subsequent Monte-Carlo simulation of the BEEM spectra. Quantitative information of the electron distributions at metal/semiconductor (M/S) interface has been obtained and its dependence upon metal surface morphology and metal thickness have been studied extensively, from which the spatial resolution of BEEM is evaluated. This resolution is found to be influenced both by metal thickness and by the morphology of the metal surface. Consideration is given to the optimum conditions for high lateral resolution of BEEM at the metal-semiconductor interface.

Further, we have extended our simulation to include the effect of nanometre scale local potential barrier fluctuation. This small patch of lowered barrier can lead to a saddle point (or pinch-off effect) in the two dimensional electrostatic potential if the depletion zone is large[1]. However, this pinch-off effect can be removed with high doping level inside the semiconductor due to the reduction in the depletion width. We have been able to quantify the doping level required for removing the pinch-off effect. The results have been used to compare with some existing experiments and explanations.

REFERENCE:

P. Niedermann, L. Quattropani, K. Solt, A. D. Kent and Q. Fischer, J. Vac. Sci. Technol. B 10(2), P. 580, 1992.

Effect of Lattice Mismatch on BEEM Transport

T. Huang, H. D. Hallen[1] and R. A. Buhrman

School of Applied and Engineering Physics

Cornell University, Ithaca, NY 14853

Although there are still many BEEM-related issues that remain to be resolved, perhaps none is more puzzling (and controversial) than the issue of what mechanism is responsible for the apparent lack of dependence of BEEM transport on substrate orientation in a number of systems based on indirect semiconductor substrates. Despite the efforts by many researchers in this area, there is still no consensus on this issue, not even on the fundamental question of whether interface or bulk scattering plays the dominant role. Our study of the limits of BEEM resolution using hot electron modification techniques has led us to conclude that only interface effects can provide the answer; a conclusion that has also been reached recently by Ludeke and Bauer who used a different experimental approach[2]. The nature of this interface effect has yet to be established. In this presentation, we will examine one possible explanation: the effect of lattice mismatch and its impact on interfacial ballistic transport and BEEM spectra.

The original BEEM model proposed by Bell and Kaiser has achieved remarkable success in explaining the BEEM spectra of metal on semiconductor substrates which have conduction band minima that are centered in a plane parallel to the interface. With its assumption of strict conservation of transverse momentum across the metal-semiconductor interface, it fails to explain, however,

why substrate orientation of some indirect semiconductor (such as silicon) seems to have little effect on BEEM transport across the interface. This strict conservation is based on the assumption that the two lattices (of metal and semiconductor) are completely matched, thus retaining the full symmetry of the single lattice in the 2-dimensional plane parallel to the interface. It also implicitly assumes that the reciprocal 2D lattice vectors are so large as to have little effect on BEEM transport across the interface, since, strictly speaking, only transverse crystal momenta are to be conserved (i.e., transverse momenta are conserved only up to some reciprocal 2D lattice vector). On the other hand, if the assumption of full lattice matching is not satisfied, the reduced symmetry makes it improper to ignore the effect of these reciprocal 2D lattice vectors on momentum conservation in many cases and can possibly provide the explanation for the lack of substrate orientation dependence of BEEM transport. We have carried out a calculation of the effects of lattice mismatch and its consequences on BEEM transport. In particular, we find that depending on the degree of the reduction in symmetry, the effect on BEEM spectrum shape can be minimal (or none if some conditions are met). It can also lead, in some cases, to such interesting results as a small shift in the apparent BEEM threshold. For example, a transverse lattice ratio of 4:3 yields an apparent threshold shift of about 20meV.

[1]Present address: North Carolina State University, Raleigh, NC 27695.

[2] R. Ludeke and A. Bauer, Phys. Rev. Lett. 71, 1760 (1993).

The Role of Scattering in the Metal Film and at the Interface in BEEM

R. Ludeke and A. Bauer*

IBM T.J. Watson Research Center, P.O. Box 218, Yorktown Heights, N.Y. 10598

Central to the issue of modelling the collector current I_c in BEEM transport is whether or not transverse momentum is conserved. All models for current transport used in the past for data fits have tacitly assumed that transverse momentum k_t is conserved whilst an electron crosses the metal-semiconductor (M-S) interface. This clearly crass assumption is highly questionable for most real M-S system based solely on the mismatch or incoherency between the metal and semiconductor lattices, with the consequence that k_t need no longer be conserved. Thus an electron crossing the interface can assume a direction in the semiconductor that is unrelated to its direction in the metal, i.e. it is scattered at the interface. The situations is actually worse for real interfaces due to the added crystallographic imperfections and the essentially unavoidable interface reactions. Although this appears to have been recognized, attempts to explain the finite I_c for the Si(111) interface (which should be zero since no conduction band minima (CBM) for Si map onto the Brillouin zone center) in terms of a k_t-nonconserving model were discarded in favor of existing k_t-conserving models due to poor fits to experimental data [1,2] We will re-address this important issue here, demonstrating for Pd/Si(111) and Pd/Si(100) that their nearly identical I_c vs. V_T spectra (where V_T is the STM tip bias) can only be accounted for if k_t is not conserved. We arrive at this conclusion through a novel determination of the inelastic and elastic electron mean free paths (mfp) in the Pd and the demonstration that even the short elastic mfp's λ_e(~35 Å) thus obtained provide insufficient scattering to account for the observed equality of I_c's in both Si orientations for Pd film thicknesses $<\lambda_e$. We have developed an expression for the collector current that assumes non-conservation of k_t. The model is based solely on the available phase space overlap between the metallic states and the Si conduction band states projected onto the appropriate (100) or (111) interfaces. Excellent fits to the data are demonstrated for ~10 Å Pd films on Si(111) and Si(100) surfaces, for which scattering effects in the metal are almost negligible. In contrast, we have clear evidence that k_t is at least partially conserved for the coherent $NiSi_2$/Si(111) interface.

Pd films over a thickness range of 8-92 Å were deposited on n-type Si(111) or Si(100) substrates and BEEM spectra were measured over a tip bias range $0.5 \leq V_T \leq 6$ V. For a series of V_T values I_c was plotted on a logarithmic plot as a function of the film thickness w. The resulting "attenuation" curves exhibited a novel behavior: instead of the usual linear (in the logarithmic sense) decrease with w in such plots, the decay rate gradually increased with thickness and reached a linear behavior only for thicknesses exceeding ~30 Å. We have modeled this behavior in terms of statistically independent elastic and inelastic scattering events that control the transit of the electron between injection at the metal-vacuum interface and its eventual arrival at the M-S interface, with the assumption that any inelastic scattering renders an electron uncollectable in the semiconductor [3]. An expression in terms of λ_e,λ_i and w is obtained for the probability that the electron reaches the M-S interface. From excellent fits to the attenuation curves we obtain unique values for λ_e and λ_i over an energy range of 1 to 6 eV. These are shown in Fig. 1. It is now possible to model the relative I_c intensities for transport across the Pd/Si(100) and Si(111) interfaces under the assumption of k_t conservation: the highly collimated unscattered (ballistic) part of the injected current above threshold will be collected in the Si(100), but not in the Si(111), whereas a fraction f_{nb} of scattered or nonballistic part of the injected current will be collected for both Si substrate orientations. The resulting I_c as a

function of w for some values of f_{nb} are illustrated in Fig. 2, together with the expression for the (relative) current intensity as a function of the mfp's and w. Since the observed I_c for Si(111) and Si(100) are essentially identical and follow the trend of curves for Si(100) in Fig. 2, rather than the rapidly decreasing Si(100) curves for small w, we are led to conclude that scattering in the metal is insufficient to provide the momenta for electrons to reach the non-zone-centered CBM for the Si(111) interface.

From the above we infer that it is primarily the interface that provides the scattering necessary for electrons to reach the Si CBM. By assuming that the scattering at the interface is isotropic, it is readily shown [3] that the collector current is proportional to the overlap of available phase space on the Si and metal sides of the interface, modified by the energy distribution of the tip current $f_T(\varepsilon)$:

$$\frac{I_c}{I_T} = \eta \frac{m_s}{2m_m} \int_{-(V_T-V_o)}^{\infty} \frac{f_T(\varepsilon)(eV_T - eV_o + \varepsilon)}{E_F + V_T + \varepsilon} d\varepsilon$$

where η is the CBM degeneracy, V_o the threshold voltage and E_F the Fermi energy of the metal. m_s is the "projected" effective mass in the semiconductor and is dependent on the orientation of the interface. For the tip function $f_T(\varepsilon)$ we use the energy distribution for a single atom tip derived by Lang et al. [4], which is considerably narrower than that obtained with the usual planar tunneling assumption. Excellent fits to data are obtained over a broad bias range with this expression, as shown in Fig. 3. The difference in intensity between the spectra arises mainly from the difference in m_s for the two orientations (~10%) rather than from inelastic losses due to different metal film thicknesses (~4%).

[1] L.J. Schowalter and E.Y. Lee, Phys. Rev. **B 43** , 9308 (1991).
[2] L.D. Bell. W.J. Kaiser, M.H. Hecht and L.C. Davies, in Scanning Tunneling Microscopy, edited by J.A. Stroscio and W.J. Kaiser (Academic Press, Boston, 1993) Chapter 7.
[3] R. Ludeke and A. Bauer, Phys. Rev. Lett. **71**, 1760 (1993).
[4] N.D. Lang, A. Yacoby and Y. Imry, Phys. Rev. Lett. **63**, 1499 (1989).

* present address: Institut für Experimentalphysik, Freie Universität Berlin, Germany.

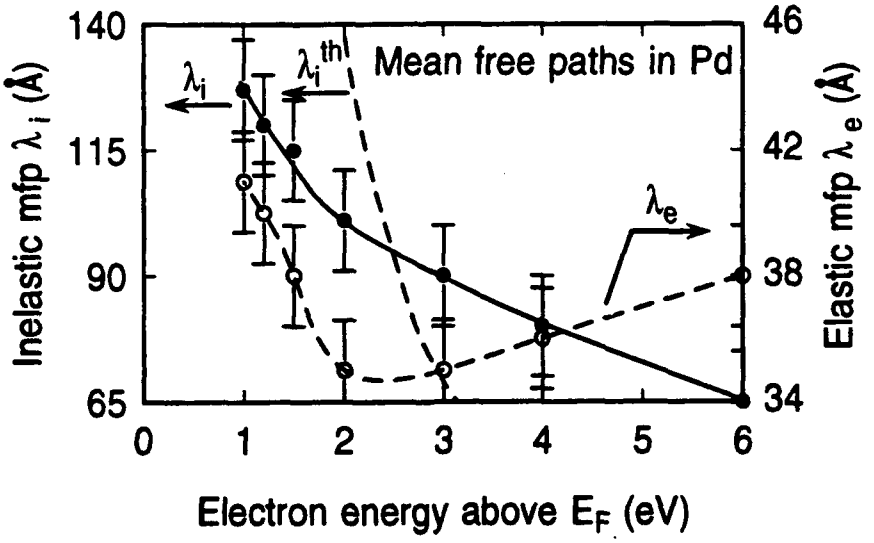

Fig. 1

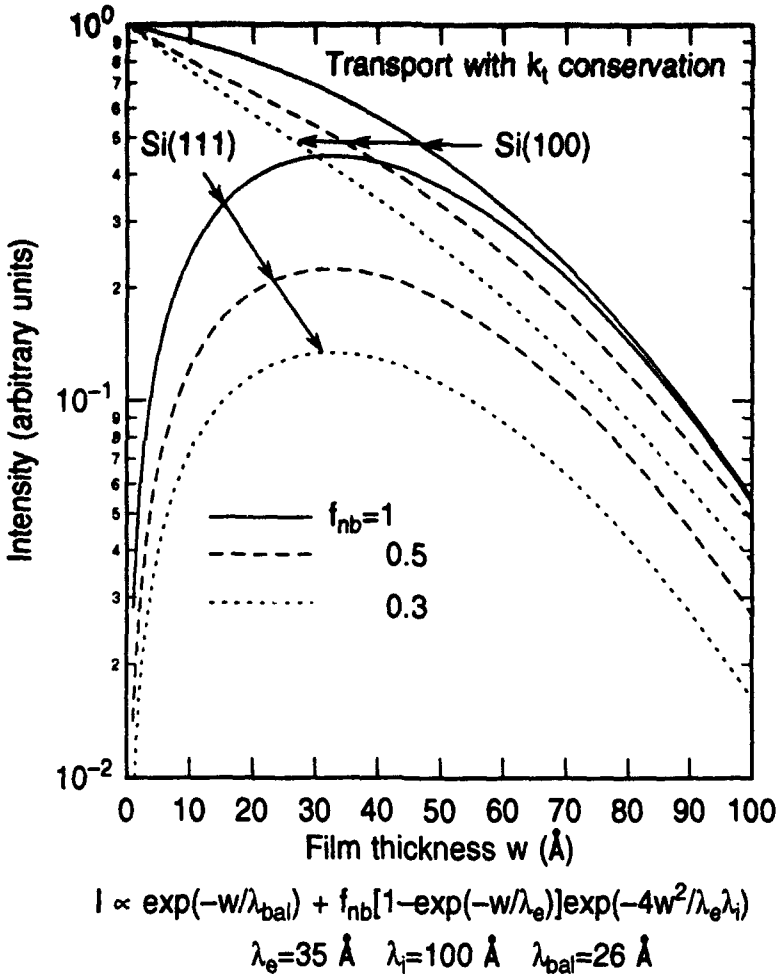
Transport with k_t conservation
Si(111)
Si(100)
Intensity (arbitrary units)
f_{nb}=1
0.5
0.3
Film thickness w (Å)
$I \propto \exp(-w/\lambda_{bal}) + f_{nb}[1-\exp(-w/\lambda_e)]\exp(-4w^2/\lambda_e\lambda_i)$
λ_e=35 Å λ_i=100 Å λ_{bal}=26 Å

Fig. 2

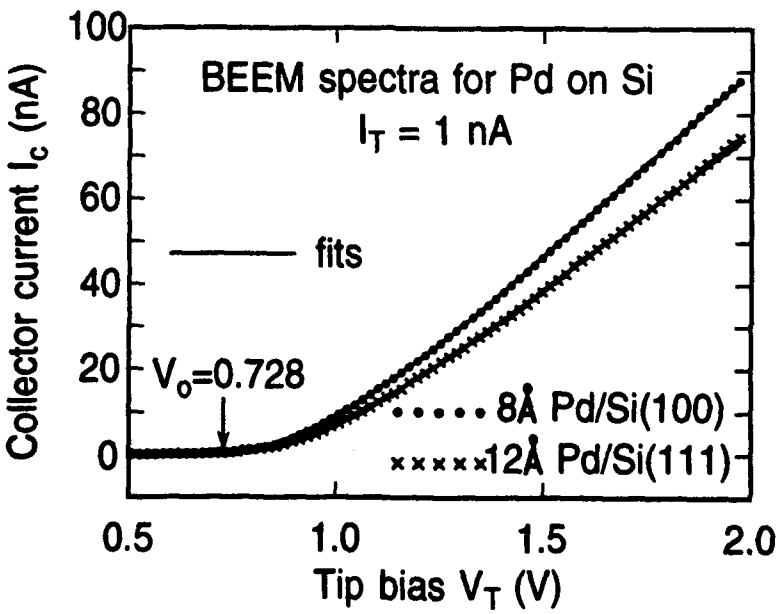
BEEM spectra for Pd on Si
I_T = 1 nA
fits
V_o=0.728
8Å Pd/Si(100)
12Å Pd/Si(111)
Collector current I_c (nA)
Tip bias V_T (V)

Fig. 3

Author Index